

**EXPERIMENTAL INVESTIGATIONS OF A MOBILE-WATER
HEATED HDH DESALINATION SYSTEM USING SOLAR
ENERGY**

BY
MOHAMMED ELMOUNZIR ISAM ELDIN BASHIR

A Thesis Presented to the
DEANSHIP OF GRADUATE STUDIES

KING FAHD UNIVERSITY OF PETROLEUM & MINERALS
DHRAHRAN, SAUDI ARABIA

In Partial Fulfillment of the
Requirements for the Degree of

MASTER OF SCIENCE
In
MECHANICAL ENGINEERING

DECEMBER 2018

KING FAHD UNIVERSITY OF PETROLEUM & MINERALS

DHAHRAN- 31261, SAUDI ARABIA

DEANSHIP OF GRADUATE STUDIES

This thesis, written by **Mohammed Elmounzir Bashir** under the direction of his thesis advisor and approved by his thesis committee, has been presented and accepted by the Dean of Graduate Studies, in partial fulfillment of the requirements for the degree of **MASTER OF SCIENCE IN MECHANICAL ENGINEERING.**

Dr. Mohammed A. Antar
(Advisor)

Dr. Zuhair Mattoug Gasem
Department Chairman

Dr. Syed M. Zubair
(Member)

Dr. Salam A. Zummo
Dean of Graduate Studies

Dr. Atia E. Khalifa

(Member)

13/5/149

Date



© Mohammed Elmounzir Bashir

2018

To my family and friends

ACKNOWLEDGMENTS

Thanks and praise be to Allah, for giving me the strength, power and will to reach where I am right now. This thesis is the culmination of my Master's degree from September 2015 through December 2018. Under the umbrella of the Department of Mechanical Engineering at King Fahd University of Petroleum and Minerals under the direct supervision of Dr. Mohammed A. Antar.

First and foremost, I would like to thank my mentor and supervisor Dr. Antar for his kindness, guidance and patience, and his scientific insight that continuously steers me in the right direction. I would like to thank also Dr. Syed M. Zubair, and Dr. Atia E. Khalifa, for being my thesis committee members, and for their support and fruitful contributions.

TABLE OF CONTENTS

ACKNOWLEDGMENTS.....	V
TABLE OF CONTENTS.....	VI
LIST OF TABLES.....	IX
LIST OF FIGURES.....	XI
LIST OF ABBREVIATIONS.....	XIII
NOMENCLATURE.....	XIII
ABSTRACT.....	XV
ملخص الرسالة.....	XVI
CHAPTER 1 INTRODUCTION.....	1
2.1 The humidification-dehumidification (HDH) systems.....	4
Psychrometric Chart.....	5
2.2 HDH Systems Classifications	6
2.2.1 Closed Air Open Water (CAOW) Water Heated cycle	6
2.2.2 Closed-Water Open-Air, Water Heated (CWOA-WH) System	7
2.2.3 Closed-Air Open-Water Air Heated (CAOW-AH) System:.....	8
2.2.4 Open air open water air-heated (OAOW-AH) system:.....	9
CHAPTER 2 LITERATURE REVIEW	11
2.1 Introduction	11
2.2 Studies on Solar HDH systems.....	12
2.2.1 CAOW solar HDH system	12
2.2.2 OAOW solar HDH system.....	14
2.2.3 OACW solar HDH system	14

2.2.4 CWOA solar HDH system	15
2.3 Studies on geothermal energy HDH systems.....	16
2.4 Studies on integrated HDH systems.....	16
2.5 Studies on hybrid HDH systems.....	18
2.6 Different HDH systems design	18
2.7 Research objectives	25
 CHAPTER 3 SYSTEM DESCRIPTION.....	 27
3.1 System process description	30
3.2 System components.....	31
3.2.1 Humidifier	31
3.2.2 Dehumidifier	33
3.2.3 Solar collector	34
3.2.4 Auxiliaries.....	34
3.2.5 Measurement Instruments.....	34
3.3 System Performance Metrics.....	36
3.3.1 Gain Output Ratio (GOR):.....	36
3.3.2 Mass Ratio (MR):	36
3.3.3 Effectiveness (ϵ).....	37
3.3.4 Governing equations	38
3.4 System Performance Test	40
3.5 Test condition	41
 CHAPTER 4 RESULTS.....	 42
4.1 Introduction.....	42
4.2 Experimental results.....	44
4.3 Open cold water cycle mobile HDH system.....	44
4.3.1 The effect of top cycle temperature at the humidifier inlet (T7)	45
4.3.2 The effect of Air flow rate (m_a)	49
4.3.3 The effect of liquid to Air flow rate ratio (MR)	52
4.4 Close cold water cycle mobile HDH system.....	57
4.4.1 The effect of top cycle temperature (T7)	57
4.4.2 The effect liquid to Air flow rate ratio (MR).....	61
4.5 Experimental and Theoretical results comparison.....	67

CHAPTER 5 CONCLUSIONS & RECOMMENDATIONS	70
 5.1 CONCLUSIONS	70
 5.2 RECOMMENDATIONS	73
REFERENCES.....	75
APPENDIX A.....	81
Uncertainty Analysis	84
APPENDIX B.....	90
APPENDIX C.....	100
VITAE	103

LIST OF TABLES

Table 1: Auxiliaries.....	34
Table 2: open cold water cycle HDH system performance at humidifier feed water = 3 LPM.	81
Table 3: open cold water cycle HDH system performance at humidifier feed water = 3 LPM.	81
Table 4: open cold water cycle HDH system performance at humidifier feed water = 4 LPM.	82
Table 5: open cold water cycle HDH system performance at humidifier feed water = 4 LPM.	82
Table 6: open cold water cycle HDH system performance at humidifier feed water = 5 LPM.	82
Table 7: open cold water cycle HDH system performance at humidifier feed water = 5 LPM.	83
Table 8: close cold water cycle HDH system performance at humidifier feed water = 3 LPM.	83
Table 9: close cold water cycle HDH system performance at humidifier feed water = 4 LPM.	83
Table 10: close cold water cycle HDH system performance at humidifier feed water = 3 LPM.	84
Table 11: close cold water cycle HDH system performance at humidifier feed water = 4 LPM.	84
Table 12: Uncertainty analysis for the open cold water cycle HDH system performance at humidifier feed water= 3 LPM.	85
Table 13: Uncertainty analysis for the open cold water cycle HDH system performance at humidifier feed water= 3 LPM.	85
Table 14: Uncertainty analysis for the open cold water cycle HDH system performance at humidifier feed water=4 LPM.	86
Table 15: Uncertainty analysis for the open cold water cycle HDH system performance at humidifier feed water= 4 LPM.	86
Table 16: Uncertainty analysis for the open cold water cycle HDH system performance at humidifier feed water= 5 LPM.	87
Table 17: Uncertainty analysis for the open cold water cycle HDH system performance at humidifier feed water= 5 LPM.	87
Table 18: Uncertainty analysis forthe close cold water cycle HDH system performance at humidifier feed water= 3 LPM.	88
Table 19: Uncertainty analysis for the close cold water cycle HDH system performance at humidifier feed water= 4 LPM.	88
Table 20: Uncertainty analysis for the close cold water cycle HDH system performance at humidifier feed water= 3 LPM.	89

Table 21: Uncertainty analysis for the close cold water cycle HDH system performance at humidifier feed water= 4 LPM.....	89
Table 22: Test condition for open cold water cycle HDH system at humidifier feed water= 3 LPM.29/7/2018.	90
Table 23: Test condition for open cold water cycle HDH system at humidifier feed water= 3 LPM. 18/7/2018.	91
Table 24: Test condition for open cold water cycle HDH system at humidifier feed water= 4 LPM. 4/8/2018.	92
Table 25: Test condition for open cold water cycle HDH system at humidifier feed water= 4 LPM.9/8/2018.	93
Table 26: Test condition for open cold water cycle HDH system at humidifier feed water= 5 LPM. 11/9/2018.	94
Table 27: Test condition for open cold water cycle HDH system at humidifier feed water= 5 LPM. 31/12/2017.	95
Table 28: Test condition for close cold water cycle HDH system at humidifier feed water= 3 LPM.25/3/2018.	96
Table 29: Test condition for close cold water cycle HDH system at humidifier feed water= 4 LPM.....	97
Table 30: Test condition for close cold water cycle HDH system at humidifier feed water= 3 LPM.....	98
Table 31: Test condition for close cold water cycle HDH system at humidifier feed water= 4 LPM.....	99

LIST OF FIGURES

Figure 1: Desalination classification based on technology.....	2
Figure 2: Rain cycle [3].	4
Figure 3: HDH system configuration-water heated cycle.....	5
Figure 4: System process on Psychrometric Chart.	5
Figure 5: Closed air open water- water heated cycle.....	7
Figure 6: Closed water open-air -water heated cycle.....	8
Figure 7: Closed air open water -air heated cycle.....	9
Figure 8: Open air open water- air heated cycle.....	10
Figure 9: System photo.	28
Figure 10: The system under investigation.....	29
Figure 11: System font view.....	32
Figure 12: System inside section.	32
Figure 13: System backside view.	33
Figure 14: Side and front view of the humidifier.	38
Figure 15: Side and front view of the Dehumidifier.....	39
Figure 16: Solar collectors.....	40
Figure 17: cold water cycles.	43
Figure 18: Open cold water cycle mobile HDH system.	45
Figure 19: The effect of top cycle temperature at $m_a = 0.075 \text{ kg/s}$ on system performace	47
Figure 20: The effect of top cycle temperature at $m_a = 0.09 \text{ kg/s}$ on system performance.	48
Figure 21: The effect of Air flow rate m_a on system GOR.	50
Figure 22: The effect of Air flow rate m_a on fresh water production.....	51
Figure 23: The effect of mass ratio on system performance MR at $m_a = 0.08 \text{ kg/s}$	55
Figure 24: The effect of mass ratio MR on system freshwater production at $m_a = 0.06 \text{ kg/s}$	56
Figure 25: Close cold water cycle mobile HDH system.....	57
Figure 26: The effect of top cycle temperature T7 at $m_a = 0.048 \text{ kg/s}$ on GOR.	59
Figure 27: The effect of top cycle temperature T7 at $m_a = 0.03 \text{ kg/s}$ on GOR.	60
Figure 28: The effect of Air flow rate m_a on system GOR. a) b)	62
Figure 29: The effect of Air flow rate m_a on freshwater production m_d	63
Figure 30: The effect of mass ratio MR on system performance at $m_a = 0.048 \text{ kg/s}$	65
Figure 31: The effect of mass ratio MR on system performance.	66
Figure 32: Theoretical and experimental results for the open cold water cycle HDH system.	68
Figure 33: Theoretical and experimental results for the close cold water cycle HDH system.	69
Figure 34: Thermocouple. [70]	100

Figure 35: Flow meter. [71].....	100
Figure 36: Weather meter. [72].....	101
Figure 37: Digital thermometer. [73].....	101
Figure 38: Rotary Thermocouple Selector Switches. [74].....	102

LIST OF ABBREVIATIONS

Nomenclature

A	Duct cross area
h	Enthalpy, kJ/kg
m	Mass flow rate, kg/s
P	Pressure, KPa
Q	Water volume flow rate LPM
T	Temperature, °C
t	Time min
RH	Relative humidity, dimensionless
V	Water volume mL
v	Air speed m/s

Greek Symbols

ω	Absolute humidity, kg H ₂ O/kg dry air
ϵ	Effectiveness

Subscripts

a	air
b	Brine
bp	Bypass water
cw	Cold water
d	Distilled water
dh	Dehumidifier
exp	Experimental
fg	Latent heat of vaporization, kW/m ² °C.

h	Humidifier
w	Hot water
status conditions	
1	At Hot water tank
2	Water After the first solar collector
3	Water from Hot water tank to the second solar collector
4	Water At the second solar collector inlet
5	Water At the second solar collector tank
6	Water at the left humidifier inlet
7	Water at the right humidifier inlet
8	Water entering left dehumidifier from the cold tank
9	Water entering right dehumidifier from the cold tank
10	The cold water after leaving the left dehumidifier
11	The cold water after leaving the right dehumidifier
12	Air at humidifier inlet
13	Air at left humidifier outlet
14	Air at right humidifier outlet
15	Air leaving the left dehumidifier
16	Air leaving the right dehumidifier
17	The hot water after leaving the right humidifier (Brine)
a1	Inlet air at humidifier
a2	Outlet air from the humidifier & inlet the dehumidifier
a3	Outlet air from the dehumidifier

ABSTRACT

Full Name : [Mohammed Elmounzir Isam ELdin Bashir]
Thesis Title : [EXPERIMENTAL INVESTIGATIONS OF A MOBILE-WATER HEATED HDH DESALINATION SYSTEM USING SOLAR ENERGY]
Major Field : [Mechanical engineering]
Date of Degree : [December,2018]

Humidification dehumidification systems (HDH) one of the types of desalination system which are known for the possibility to operate using renewable energy at low temperature and also need low initial, maintenance and operating cost.

In this study, an experimental and a theoretical investigation on two configurations of a compact mobile HDH water heated system using water heating solar collectors are presented. The effects of different operating parameters such as top cycle temperature, air flow rate, and water-air mass ratio on system performance are shown. Experimentally, the maximum GOR recorded was 0.35 at a humidifier water flow rate of 5 LPM and 1.1 water-to-air mass flow rate ratio (MR). The maximum fresh water produced was 4.7Kg/hr at a humidifier water flow rate of 4 LPM and 1.2 water-to-air mass flow rate ratio (MR).

Finally, a new modification is presented for the system based on the drawbacks that appear during operating the system which can be tested in future work.

ملخص الرسالة

الاسم الكامل: محمد المنذر عصام الدين بشير حامد

عنوان الرسالة: فحوصات تجريبية لنظام تحلية المياه التبخري التكتيفي المتحرك الذي يستخدم الطاقة الشمسية.

التخصص: هندسة ميكانيكا

تاريخ الدرجة العلمية: ديسمبر 2018

الأنظمة التبخرية التكتيفية أحد أنواع نظم تحلية المياه التي تتميز بامكانية استخدام الطاقة المتجدددة عند درجة حرارة منخفضة ، وتحتاج إلى تكلفة بناء و تشغيل وصيانة منخفضة.

في هذه الدراسة ، تم إجراء بحث تجريبي ونظري على نوعين مختلفين من الأنظمة التبخرية التكتيفية المتحركة التي تستخدم الطاقة الشمسية لتسخين المياه ، مع بيان تأثير العوامل المختلفة مثل درجة حرارة الدورة العليا ، ومعدل تدفق الهواء ، والسبة بين كتلة الماء والهواء على أداء النظام .

من الناحية التجريبية ، كان أقصى GOR مسجل يعادل 0.35 عند معدل تدفق ماء المرطب يساوي 5 ليتر/دقيقة و 1.1 نسبة تدفق الماء إلى الهواء (MR) ، والحد الأقصى للمياه العذبة المنتجة كان 4.7 كجم / ساعة عند معدل تدفق ماء المرطب يساوي 4 ليتر/دقيقة 1.2 معدل تدفق كتلة الماء إلى الهواء.(MR)

وأخيراً، تم تقديم تعديلات على النظام بناءً على العيوب التي ظهرت أثناء تشغيل النظام السابق، ويمكن ان تدرس هذه التعديلات في العمل المستقبلي.

CHAPTER 1

INTRODUCTION

Clean water shortage is considered to be one of the most important issues nowadays.

By 2025 as the result of the population increasing, many countries will suffer from fresh water scarcity which is only available on rivers and groundwater.[1].

Although water covers most of the Earth (oceans), unfortunately, only less than 2.5 % of earth water supply is fresh water while 97.5% of earth water is seawater. Almost 80% of earth fresh water is frozen as icecaps and it is hard to access for the human's use. For that reason, there is an urgent need for desalination as a way to solve that major problem.

Desalination process is defined as a process that separates salts from water. A desalination process separates saline water into two product. The first product is water with low or no salt concentration compared to the original feed water. This is the main objective of desalination and it called desalinated or distilled water. The second part is water with a high salt concentration usually referred to as brine.

Desalination is one of the oldest and most commonly used water treatment technology. Based on technology desalination can be classified into categories **figure 1, thermal desalination process** (evaporation and condensation process) which follows the same principle of rain cycle, and **membrane desalination process** which follows the idea of force. By using a membrane material (a semi-impermeable thin layer which allows

only pure water particles to pass through) and applying some pressure, only pure water will migrate to the other side and collected as fresh water.

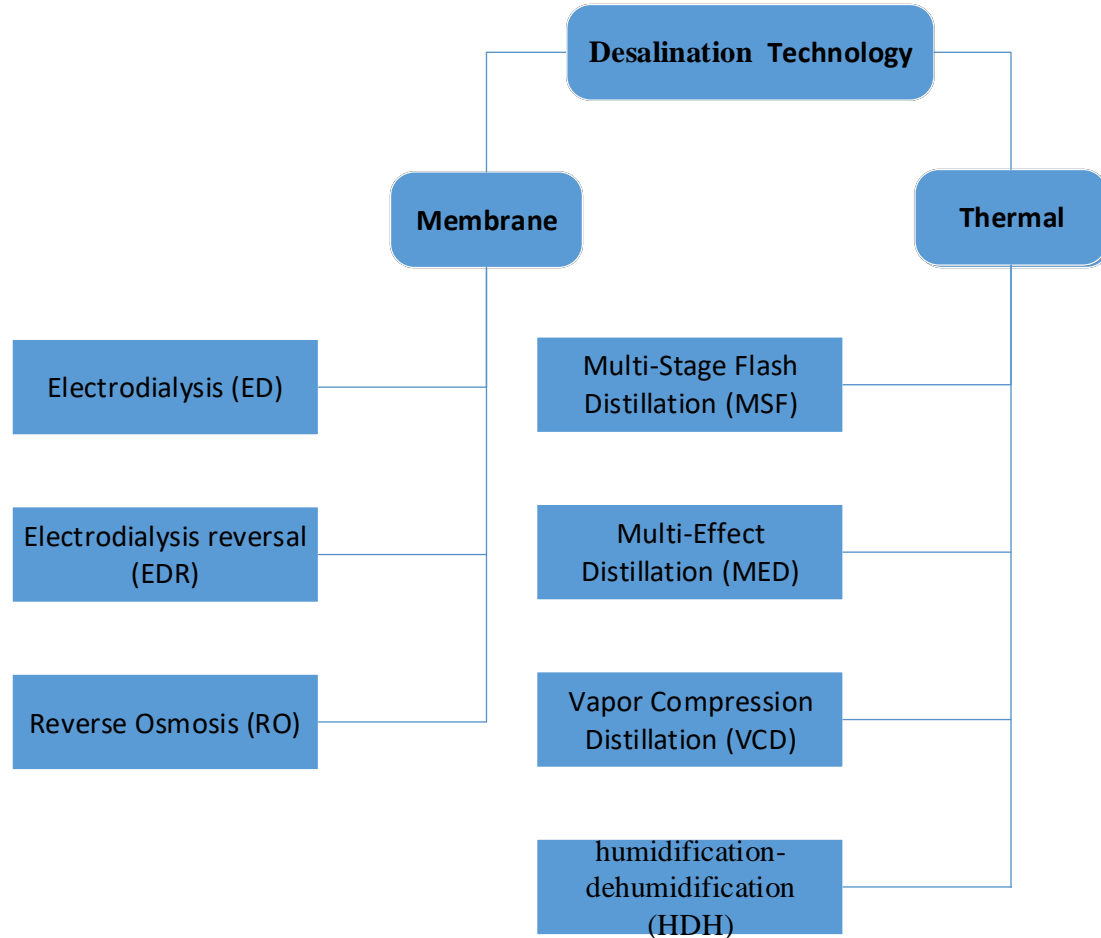


Figure 1: Desalination classification based on technology.

Most of the thermal desalination systems are designed with evaporation process technology (rain cycle). The rain cycle starts when the water evaporates due to solar radiation, which heats the salty water on the surface of oceans to higher temperatures. Therefore, the density of evaporated water becomes lower, air carries the evaporated water above the earth surface (humidification process). Then, humid air forms clouds, which travel due to the effect of wind, until they reach cold regions, wherein if the temperature of the humid air is lower than the dew point. Finally, the vapor comes down and starts to condensate in the form of rains (dehumidification process). [Figure 2](#) [2] illustrates the whole rain cycle.

Thermal desalination is a man-made cycle of rain, instead of solar radiation we can use any source of energy such as electrical energy, nuclear energy, and geothermal energy. For the humidification-dehumidification process, we can use devices that simulate the same procedure, for example, the evaporator (humidifier) and the condenser (dehumidifier).

Desalination plants produce about 77.4 million cubic meters per day [2] around the world using, MSF (Multi-Stage Flash) and RO (Reverse Osmosis) processes are the most common techniques for desalination, due to the ability to have very large production. However, there is a rising interest in using MED (Multi-Effect), HDH (humidification–dehumidification) and membranes as desalination techniques, since they showed small capacities, which could be used effortlessly in remote areas.

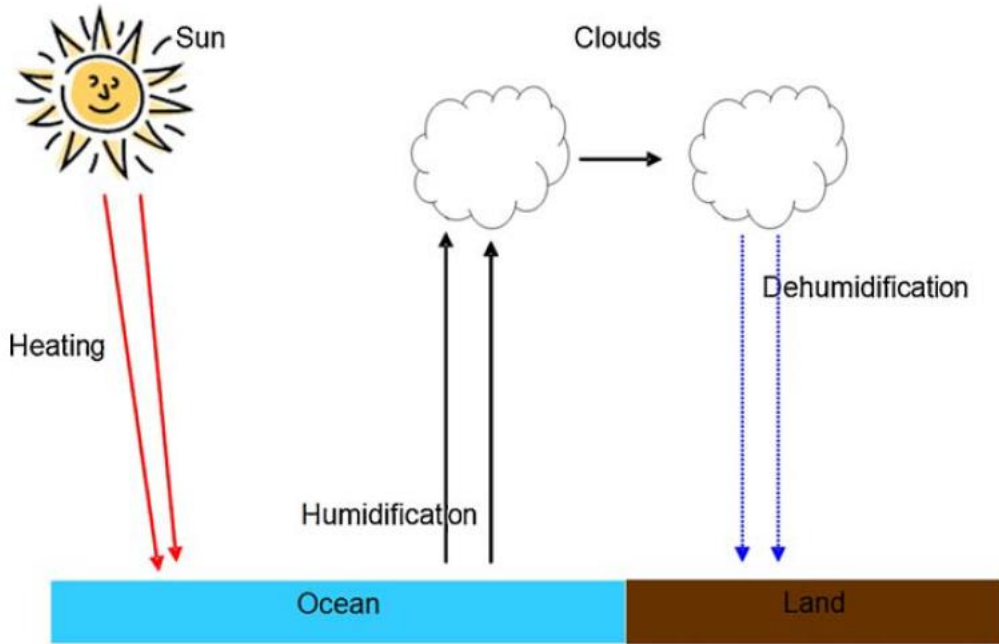


Figure 2: Rain cycle [3].

2.1 The humidification-dehumidification (HDH) systems

Basically, an HDH system consists of three parts as shown in [figure 3](#), the first part is the humidifier or the evaporator, wherein, the humidity of air increases to the saturation condition. The second part is the dehumidifier or the condenser, which is used to cool humid air and condense water vapor. The last part is the energy unit, namely: heater, which is used to heat either the air or the water.

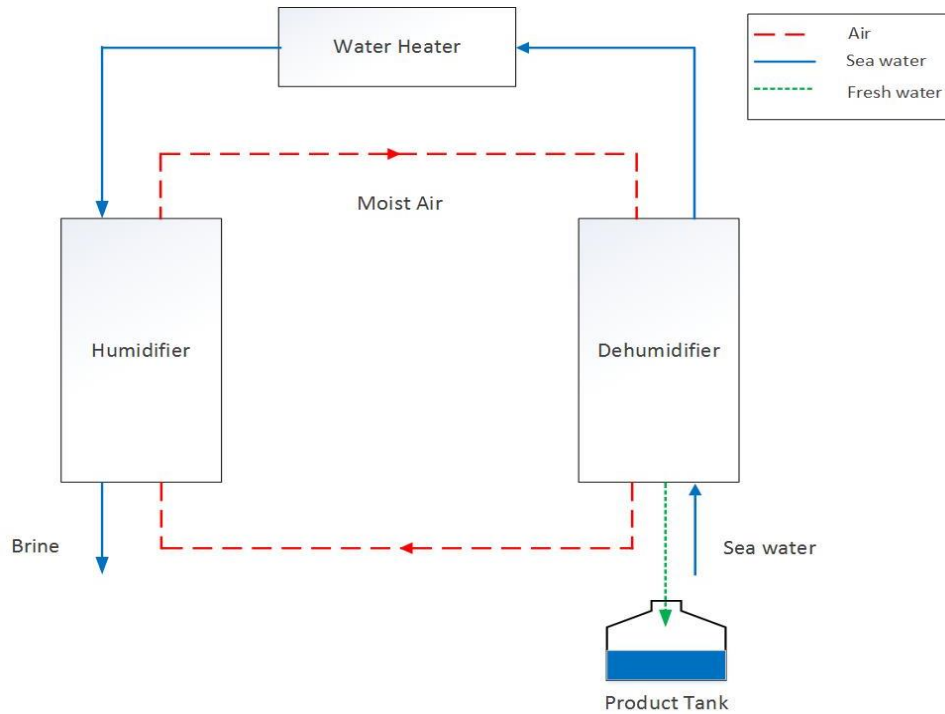


Figure 3: HDH system configuration-water heated cycle.

Psychrometric Chart

One way to explain the HDH system is to present on the psychrometric chart which follow the air process and clarify it. At first on this system the air is heated and humidified in the humidifier, lastly, it cooled and dehumidified on the dehumidifier. [Figure 4](#).

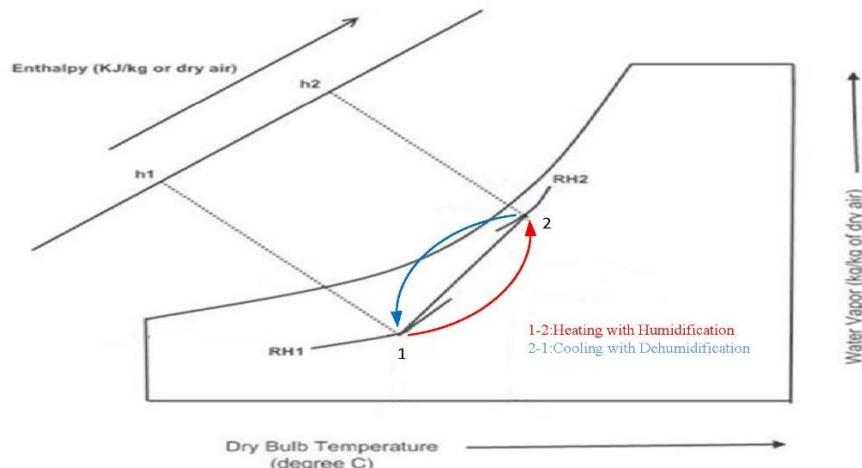


Figure 4: System process on Psychrometric Chart.

2.2 HDH Systems Classifications

HDH systems categorized according to:

- 1- Whether air or water is heated.
- 2- The type of air or water circuit (open or closed loop).
- 3- Based on the source of energy used (solar, thermal, geothermal and hybrid).

2.2.1 Closed Air Open Water (CAOW) Water Heated cycle

In this system, the seawater enters first into the dehumidifier which is basically a heat exchanger, wherein it the seawater is preheated by the hot humid air (moist air) coming from the humidifier so, the humid air cools down. As a result of that the vapor carried by the humid air start to condense (fresh water) when the temperature drops to a temperature which is less than the dew point temperature (condensation process). Meanwhile, seawater is heated thus recovering some energy given by condensing vapor, then it is further heated in the heater to a high temperature. Lastly, the hot seawater (feed water) enters the humidifier where it is sprayed and mixed with the cold air coming from the dehumidifier. Therefore, some of the seawater evaporates and carried by air that is heated and humidified while the remaining seawater in the humidifier is rejected as brine and air stream circulate to the dehumidifier to complete the closed loop. [Figure 5](#) shows the cycle.

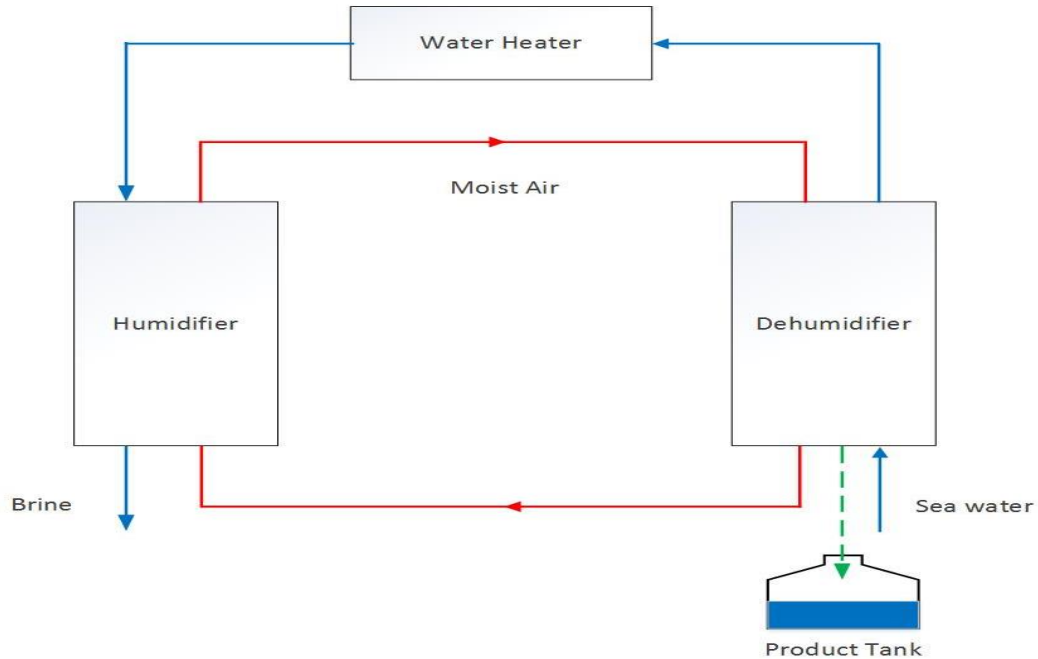


Figure 5: Closed air open water- water heated cycle.

2.2.2 Closed-Water Open-Air, Water Heated (CWOA-WH) System

The sea water is preheated in the dehumidifier by the heat which transfers from the humid air, then drier air is released to the ambient. After that, the seawater is heated again in the heater, then some of the heated seawater, which is sprayed at the humidifier evaporated after it mixes with entering the air. The remaining sea water which does not evaporate in the humidifier circulates again to the dehumidifier (closed loop). An illustration of this cycle is given in [figure 6](#).

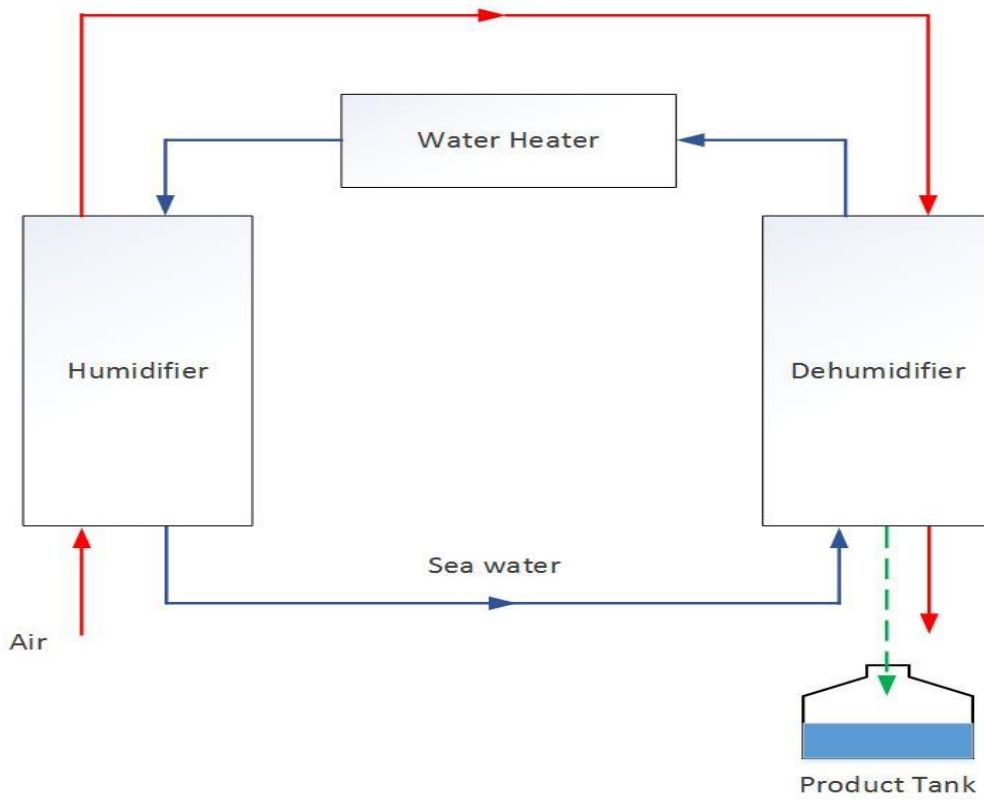


Figure 6: Closed water open-air -water heated cycle.

2.2.3 Closed-Air Open-Water Air Heated (CAOW-AH) System:

Air is heated by the air heater to a high temperature and then entered the humidifier where it is cooled and saturated. Lastly, the air dehumidified and condenses out the water vapor carried by air at the dehumidifier as shown in [figure 7](#).

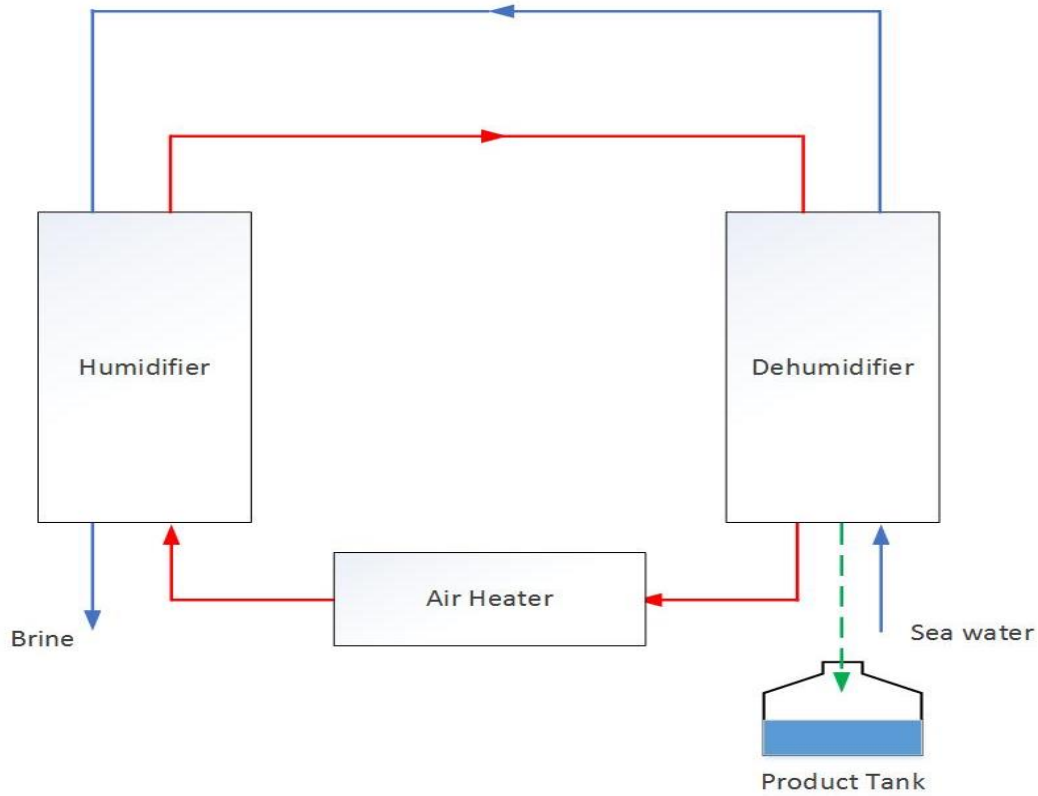


Figure 7: Closed air open water -air heated cycle.

2.2.4 Open air open water air-heated (OAOW-AH) system:

Another type of HDH systems is Open-air, open-water (OAOW) air heated cycle, this cycle operates in the same way as the closed air system. There are only two differences, the first difference is that air is heated by the heater after it exit the humidifier. For the air cycle, the air rejected to the atmosphere after it leaves the dehumidifier and only fresh air from the atmosphere enter the humidifier is the second difference. It is illustrated in [figure 8](#).

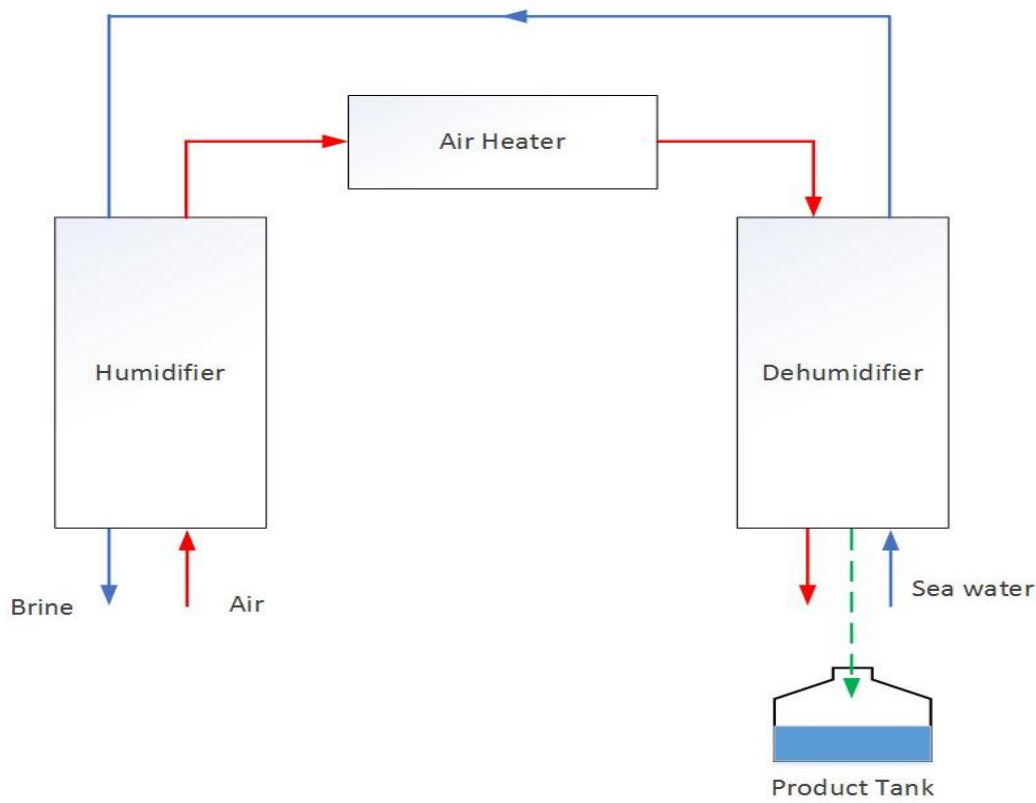


Figure 8: Open air open water- air heated cycle.

CHAPTER 2

LITERATURE REVIEW

2.1 Introduction

In spite of the fact that the majority of desalination plants worldwide are large-scale plants, which are inconvenient for developing countries and remote locations as a result of their:

- High initial and operation cost because of high materials requirements and Huge energy consumption (fossil fuels for thermal plant and electrical energy for membrane plants).
- Ecological footprints due to high carbon dioxide emissions, which results in serious danger to the environment.

For all of these reasons, the importance of developing desalination techniques that can operate using renewable energy likewise inexpensive (easy to construct and low maintenance needs) such as HDH systems arises. They are suitable not only for rich countries but also for developing countries[4].

The economic and environmental benefits are one of the main advantages of HDH systems especially when low to medium scale fresh water production is needed. Also, HDH technology distinguishes from other desalination technologies with the ability to operate at low temperature, the possibility of running system using different source of energy (solar, geothermal and electrical energy), easy constructing of the system and low requirement for

system maintenance, all these motivates many researchers for more investigation of this technology.

Most of the studies are concerned with the efficiency and productivity improvement by changing energy source especially solar and geothermal energy, altering system components design, integrating HDH with mechanical devices and lately combined HDH process with other desalination techniques (hybrid systems).

2.2 Studies on Solar HDH systems

The studies performed on solar HDH can be categorized based on the type of air-water cycles to:

2.2.1 CAOW solar HDH system

One of the first investigations on CAOW HDH system with solar collector was made by Al Hallaj et al [5]. On the water heated system, the feed water is preheated by the latent heat of condensation which reduces the amount of energy needed from solar collectors and enhances the efficiency. For that reason the system capital cost was reduced compared with similar system working with conventional energy sources.

After that, many attempts for improving the system performance was made on CAOW system by many researchers. For examples, Chafik [6] studied the same design but in his system, air is heated instead of water. Moreover, Farid and Hamad [7] fabricated a HDH system that produced 12 L/d.m^2 of solar collector area (which was approximately three times the production using a solar still with the same solar conditions). However, the system faced two main drawbacks, the high-pressure drop in both the humidifier and dehumidifier and high electrical power consumption due to the blower. Furthermore, an experimental

study presented the effect of water to air ratio on the performance of the system was carried by Farid et al. [1] and Al-hallaj et al. [5]. They found the optimum water air ratio for their system which gave the best performance (The maximum performance were 12 L/m^2 per day and GOR around 4 for Farid et al and 8 L/m^2 per day with a GOR close to 2 for Al-Hallaj et al). At last, they recommended using forced air circulation for good performance at a low top temperature.

Muller-Holst et al. [8] presented CAOW HDH water heated system with thermal storage tank constructed in Tunisia. The reported results indicated that the production rate was 500 Liters per day, system GOR was between 3 and 4.5 and the thermal storage tank reduced the cost of water production by 50%.

A mathematical model was carried out for normal CAOW HDH water heated system, the simulation data based on thermo-economic analysis showed that system had 99.05 kg/h of freshwater production and a GOR about 1.5. The model indicated that the system GOR may improve to 1.85 when system components effectiveness increase to 0.9 [9].

An experimental setup of single stage HDH system with solar collectors gave production rate equal 10 Liters per hour introduced by Soufari et al.[10]. Also, a theoretical study for designing a solar CAOW HDH water heated system which can operate even at night in the absence of solar radiation carried out by Yuan et al [11]. A mathematical model was developed for the system to predict the performance. The Results showed the effect of air flow, solar collector surface area, feed water, cooling water and system dimensions on both freshwater production and system efficiency. Furthermore, the system produced $5.2 \text{ kg/m}^2 \text{ d}$ in summer while in winter only $2.7 \text{ kg/m}^2 \text{ d}$ was produced.

Zhani and ben Bacha [12] investigated CAOW single stage HDH system with both air and water heating. The system gave average production rate equal 17 liters per day. 9 liters per day is the production of CACW single stage HDH system with both water and air heating design and tested experimentally by Nafey et al [13].

2.2.2 OAOW solar HDH system

Ben Bacha et al. [14] carried out an investigation on OAOW solar HDH system with a storage tank, this included modeling, computer simulation, and experimental validation. Their research showed that the water production was 19 liters per day with a GOR less than 0.5. Besides, the presented system data predicted that increasing hot water temperature and flow rate inside the humidifier while decreasing the temperature of cold water at dehumidifier and recycling the brine to the humidifier will improve system performance. Also, the system storage tank saved 16% solar collector area.

The humidifier inlet water temperature together with the heat losses from both the humidifier and the dehumidifier are the main factors for estimating the system performance which was concluded experimentally and theoretically By Garga et al. [15] when they investigated multi-effect OAOW Solar HDH system with 5 liters thermal storage tank capacity.

2.2.3 OACW solar HDH system

OACW HDH air heated system with solar collector as a source of heat simulated using theoretical model presented by Yamal and Solmus.[16], then for the same system Orfi and Laplante [17] proved that the fresh water production depends on the air-water mass ratio. After that, a modification of the system had been made on the main equipment and examined theoretically and experimentally by Nafey et al. [18]. They found that the

performance is strongly effected by the temperature inlet in both humidifier and dehumidifier, air water ratio, solar intensity and wind speed. Finally, they reported that the maximum production for the system was 9 Liter per day and higher air mass flow results in less productivity because it reduces the humidifier inlet temperature.

Dai et al. [19] found that the system performance depends on the humidifier inlet temperature and water – air ratio. It was noticed from the results that there is an optimum air velocity for each hot water flow rate, and the major factor which affects the production of fresh air is the top hot water temperature. A HDH system using solar collectors was designed and tested experimentally under various weather condition by Dayem [20].

2.2.4 CWOA solar HDH system

For CWOA HDH water heated system, Al-Enzi et al. [21] investigated the influence of changing hot water temperature, cold water temperature, and water – air ratio on the system production. They concluded that the production growth with the increase of the hot water and air mass flow rates. On the other hand, the decrease in water mass flow rate and cooling water temperature improved system production.

X li et al [22] performed an experimental study on single stage CWOA HDH system with solar collectors. The system produced 0.77 L/h for each 1m² of the solar collector area and have GOR equal to 2. Also, Yuan et al [23] modified the same system into OWOA HDH system and did an experimental investigation. The system made 1000 liter daily of fresh water and have GOR about 2.3.Mohamed AMI et al [24] designed a theoretical model for optimizing water production for CWOA HDH water heated system by using parabolic trough solar collector as the source of heat. The results showed that the system water

production had increased also, the maximum productivity was obtained during the summer season.

2.3 Studies on geothermal energy HDH systems

An HDH system using geothermal energy instead of solar collectors was developed by Bourounia et al. [25]. In addition, a study has been made to observe the ability of using geothermal energy for heating the feed water for HDH system [26]. Then, Mohamed AMI et al [27] investigated experimentally and theoretically the effect of air to water mass flow ratio, cooling water temperature and temperature of geothermal heat source on distilled water production and system performance. It was noticed that the system had the best result at air-water mass flow ratio between 1.5 and 2.5. Besides, increasing geothermal heat source temperature improved the fresh water production as result of increasing temperature difference to the cooling water inside the dehumidifier.

2.4 Studies on integrated HDH systems

Vlachogianniset al [28] developed combined desalination system using HDH model and mechanical vapor compressor. One of the drawbacks they found on that system was the large amount of air and vapor needed to run the compressor. Furthermore Narayan et al [29] modified water heated HDH system by adding mechanical compressor that was used to rise humid air pressure so, make it easier to increase air temperature at high pressure. A comparison between the modified system performance and the regular HDH system showed that the modified system had a GOR around 6, which was three times more than the GOR of normal HDH system.

An HDH system with 8.88 GOR presented theoretically by Lawal et al [30]. This high performance was achieved as result of adding a heat pump cycle to modified air heated HDH system. So, the heat pump refrigerant absorbs heat from the seawater that enters the dehumidifier (the cold water used to condense water vapor) during one part of the cycle, and at the other part of the cycle rejected heat from the condenser is used for heating the humid air coming from the humidifier. Moreover, the mathematical model indicated a growth in the humidifier and dehumidifier effectiveness as result of increasing system heat recovery by the heat pump. Furthermore, the effect of air-water mass flow rate, feed water cycle temperature and refrigerant flow rate on both system performance and water productivity were presented.

Following the same idea of adding a heat pump to HDH system, a system with distilled water production and GOR equal 2.79Kg/h and 2.08 respectively was showed from the experimental analysis [31]. Also, the same system gave 5.14 and 1.24 GOR with 82.12 and 12.75 Kg/h water production when theoretical analysis carried by He and Xu [32]&[33].

Integrated solar photovoltaic cells (PV) with HDH system was investigated by Giwa et al[34]. Inlet dry air passes over PV cells before entering the humidifier, so it can gain the heat generated from PV cells during the process of transfer the absorbed solar radiation to electrical power. This heat is used to preheat the air resulting in not only enhancing the system performance, but also generating electrical power from the PV cells. The system Produces $833 \text{ L/m}^2 \text{ y}$ of fresh water and generates 278 kWh during lifetime analysis. At last, they realized that the variation of solar radiation intensity cased high fluctuation in freshwater production, therefore they advised adding a battery to the system so that the extra electricity can be stored and recovered when needed. Also, an alternative

energy source can be added to the system as a back-up in case that solar energy is not enough to operate the system.

2.5 Studies on hybrid HDH systems

An effort was made to produce large-scale freshwater using HDH technique by integrating it with other systems such as desalination technologies (Reverse osmosis (RO) and single stage flashing (SSF)) and air conditioning systems. Combined HDH system with RO investigated by Narayan et al.[35]. They used high-pressure steam as the source of heat, the reported RO-HDH system had GOR of 20, which is higher than the performance of both HDH and RO individual system.

Franchini et al [36] investigated the idea of combining close air cycle water heated HDH system with a solar cooling plant. Instead of rejecting a large amount of heat at low temperature to environment from the cooling plant absorption chiller, it can be used as a source of energy for the HDH system to heat the feed water before entering the humidifier. This modification increased the performance for both cooling plant and HDH system in term of cooling load and freshwater production and reduced the system cost by (7-28%). The result of reducing the absorption chiller cooling water temperature increased the amount of heat can be rejected (cooling load). Moreover increasing feed water temperature made it possible to raise the amount of feed water flow rate inside the humidifier, which affects directly the growth in freshwater production.

2.6 Different HDH systems design

Khedr [37] was one of the first researchers who made a change in the dehumidifier design, a HDH system with a direct contact dehumidifier (packed tower) was presented by him. He showed that the system GOR is 0.8 and the production rate is about 10000 liter per day.

Zubair et al [38]. Studied the effect of changing the geographical location on the performance of CAOW solar HDH system in five major cities in Saudi Arabia (Dhahran, Jeddah, Riyadh, Sharurah, Qassim, and Tabuk). Also the influence of altering the number of solar collectors and system components effectiveness was presented. Moreover, the maximum freshwater production made by the system located in Sharurah and it was 19.445 L, in contrast, Dhahran scored the lowest water productivity about 16.430 L. Furthermore \$0.032 to \$0.038 was the range of price per liter of freshwater in all cities. Also, a detailed research on the performance of different HDH system in many locations in the world carried out by Bourounia et al.[39], they recommend to run the distillers at low temperature to avoid running them under vacuum condition.

A flat-plate solar collector with 1.15 m^2 surface area was used to supply the system with a hot water for humidification process, the system production of distilled water was 9 liter/day for each 1m^2 of solar collector surface area. Also, he noticed that the feed water temperature play a major role in system performance and the distilled water cost 0.5 USD for each liter which it may consider expensive compare with other systems.

Muthusamy and Srithar [40] thought about reducing the system heat losses by increasing the heat transfer area for each system component. Then, the modified system performance was tested after placing two types of packing materials inside the humidifier and emerging many types of inserts at different positions with different pitch ratio (PR) inside both air heater and dehumidifier. The study reported that the best system performance achieved when short-length twisted tape inserts, spring inserts and gunny packing material are used inside the air heater, the dehumidifier and the humidifier respectively, and with

air heater and the dehumidifier with pitch ratio equal 3. Additionally, the modified HDH system gave 11.23 kg/h m^2 freshwater productivity which is more than the productivity of normal HDH system with the same operation condition by 45%.

A thermodynamics mathematical model was developed to compare the performance of air heated and water heated HDH system with changing systems component's size (heater, humidifier, and dehumidifier)[41]. The study showed that the effectiveness of both the humidifier and the dehumidifier increased proportionally with system component's size resulting in improving system GOR. Also, raising the temperature of feed water entering the humidifier enhances the system GOR for air heated cycle, in contrast, it drops system GOR for water heated cycle. Finally it is observed that both configurations gave almost the same performance when they were exposed to the same operating condition. The differences between air heated cycle and water cycle with same performance come from the need for larger size humidifier than dehumidifier for the air heated cycle, which is opposite in the water heated cycle that used a humidifier smaller in size than dehumidifier.

Nawayseh et al. [42] studied three HDH systems with different humidifier and dehumidifier design placed in Jordan and Malaysia. They noticed that the water flow rate plays an important role in the design of the wetting area of the packing materials, the natural circulation gives a better performance than forced circulation and the maximum water production was 5 Kg per hour. Klausner [43] designed HDH cycle with a direct contact packed bed dehumidifier which is used to recover part of water production heat in a separate heat exchanger.

Also a system with water production around 5 Kg per hour and GOR about 4 was introduced by Nawayseh et al. [44]. It is a single stage HDH system with heat recovery unit in the condenser. Zamen et al. [1] presented a mathematical model that shows how changing the system parameters affect the performance of that system, also the optimum running condition that gives the maximum water production which was (10 l/hr). After that, they added a solar part and economic analysis for their model [45].

Zamen et al. [46] examined experimentally the influence of system parameters on multi-stage HDH system and compared it with single stage HDH system. They found that multi-stage technique showed good improvement (the water productivity was 7.25 l/day/m^2).

Garga et al [15] studied experimentally a single stage HDH system with heat recovery at the dehumidifier which gave 3.15 L/hr.m^2 . Then a HDH system that uses an electrical heater was presented by Amer et al [47]. This system produced 9 liters per day of fresh water and have maximum GOR about 0.6.

Hou et al. [48], created a new method to find the optimum air -water ratio and also maximize the condenser heat recovery using the pinch technology for enhancing system performance. However, they did not consider the solar collector efficiency and the temperature at the humidifier inlet. After that, he did the same study for two-stage solar HDH desalination system [49].

Chafik [50] design multi-stage air-heated solar HDH system, in which the humidification and heating process are done in many stages. The designed system had a high production cost which can be enhanced by reducing the pressure drop through the main units. Houcine et al. [51] did a similar system to Chafik's. They investigated multi-stage solar HDH

system. They reported that the system water production was 500 liter per day and the cost of solar collectors is about 37% of system cost.

An experimental investigation of a solar HDH air heated system with heat recovery unit carried out by Orfi et al.[52]. They showed that the maximum water production depends on the water-air ratio, which it affected by the ambient conditions too. The maximum humidification indicates the optimum water-air ratio. Moreover, a single stage HDH system with storage tank produced about 4 Kg of water per day was made by Yamali et al. [53]. They reported that the air flow rate had no effect on the system performance and the productivity of freshwater increased with the rise in both air and water mass flow rates.

A Novel HDH system that used both electrical and solar power as a source of energy studied experimentally by Elminshawy et al. [54]. System results showed that the system has 0.77 efficiency and produces 30.3 L/m^2 for each day. Dayem et al [55] presented a single stage HDH system in which water heated by solar collectors and electrical heaters. The system maximum GOR was 0.5 and the freshwater productivity was 3.7 L/m^2 daily.

McGovern et al. [56] investigated how the extraction -injection of air on two-stage HDH system influence the system performance (enhance the heat recovery) using pinch analysis. The results show improvement in the system performance due to a decrease in the temperature of the pinch point. Fath et al. [57] presented that the productivity of air heated HDH system increased as solar energy increase and wind velocity decrease. Also, they reported that the dehumidifier size does not play important role in the performance of the system.

A new technology to heat the sea water using cylindrical Fresnel lens concentrator over the humidifier on multi-stage HDH system was offered by Wu et al [58]. The experimental data showed that the system have a GOR about 2.1 at 867 W/m² solar intensity.

The used of an aluminum sheet as humidifier packing materials for open-air open water HDH water heated system was studied experimentally[59]. The system produced 15L/h with a cost of \$0.01 per liter. Besides, the effect of changing system parameters on the system performance was presented. An experimental study on a modified HDH system where both air and water heated in a special solar collector before entering the humidifier for humidification process and complete the normal cycles carried by Rajaseenivasan et al [60]. 15.23Kg/m² was the maximum freshwater productivity obtained from this system with the cost of 0.0257 \$/kg.

Solar HDH desalination system with air bubbling technique for humidification process was studied theoretically by Zhang et al [61]. The investigation concluded that humidification capacity (the evaporation water) increased with the amount of heat supplied during air bubbling process. With the same principle, an experimental investigation was carried out by Ghazal et al[62]. The study presented that the humidification process by air bubbling technique is more efficient than the normal humidification technique for solar HDH desalination system. Also, the investigation shows the influence of bubble regeneration, bubble coalescence and water temperature on system performance. Moreover, the study suggested increasing the contact surface area between the air and water inside air bubbling water-filled solar collector using inverted sieves to resize the air bubbles. In addition, the installation of a reflection devices to increase the

amount of solar radiation received by air bubbling solar collector. This improved the humidification process by 32% at an air flow rate of 12.6 kg/h.

A maximum water production (0.82 Kg/hr) was achieved from an air heated HDH system designed by Muthusamy [63], when the air flow rate was 21 kg/h and the angle of orientation of the air heater was 180°. The system air heater was modified by placing a circular half-perforated inserts inside the air heater with adjustable angles of orientation from 45° to 180°. Furthermore, an economic analysis was carried out to analyze the system feasibility, so the payback period was found to be 171 days. Finally, they recommended that merging phase change material (PCM) with the air collector to improve system performance.

The idea made by Muthusamy, which suggested merging air solar collector with PCM was tested by Summers et al [64]. They observed that as Muthusamy expected, the air solar collector efficiency increased by 35%. Unfortunately, it is not practical applying this modification on large-scale desalination system from an economy point of view due to the need for high numbers of air solar collector with huge surface area.

A modified HDH system with sub-atmospheric pressures inside the humidifier provided 3.43 GOR and 1.07 freshwater production, this improvement came mainly as result of operating the humidifier at low pressure [65]. Also, the system had maximum 8.2 GOR when the humidifier operate at 50 KPa and with 0.9 system components effectiveness[66]. Recently many studies were made focusing on optimizing the HDH system performance in term of distilled water production, energy consumption and system cost by changing system components design i.e. enhancing the efficiency of the heater, the humidifier, and the dehumidifier. So Ashrafizadeh et al [67] developed a theoretical model searching

for the reason of high heat losses in the HDH systems, depending on exergy laws using driving force concept, the analysis was done and found that the majority of heat losses came from the heater section (around 90% of system heat losses) and the heat losses from mass transfer across system components can be neglected.

Seeking for the best configuration of solar HDH system, a comparison between different types of solar HDH system made by Narayan et al. [68] based on if the water or air is heated during the cycle. It was observed by Muller et al [69] that the multi-effect closed-air open-water HDH water heated system has the best performance while the produced freshwater cost was found in the range of 3 – 7 USD/m³.

2.7 Research objectives

Looking for new ways to enhance HDH technology has been shown in the literature review. Part of these researches focus on finding a new method to improve the system heat recovery. A large portion of the heat losses comes from throwing away the brine (warm water) that exit the humidifier in the normal HDH system, instead of finding a way so it can participate in the heating process inside the heater because it has higher temperature than the feed water. One of the solution for this problem is replacing the water cycle on the normal HDH system with two water cycles. A hot water cycle (between the humidifier and heating device) and a cold water cycle (between the dehumidifier and cold water source). In this research, an experimental and theoretical investigation is performed on two water close cycles, open air cycle mobile HDH water heated desalination system with solar collector as a source of heat.

The objectives of this experimental investigation are to:

- 1- Modify a Cross flow compact mobile HDH water heated system using water heating solar collectors upon an estimate of the required number of solar collectors.
- 2- Test the proposed system and show the effect of main parameters on the productivity of the system. Such as:
 - a) Air flowrate.
 - b) Water flowrate
 - c) Liquid to air mass flowrate ratio.
 - d) Environmental parameters that change the top cycle temperature.

CHAPTER 3

SYSTEM DESCRIPTION

The proposed system is a modified water heated system to have two closed water cycles, open-air water heated cycle solar mobile HDH desalination system. The system is diagrammatically shown in [Figure 10](#). This system is built on a trolley, which means it can be taken to remote areas with seawater supply.

The system contains two water cycles, a hot water cycle between the humidifier and the solar collectors and a cold water cycle between the cold water tank and the dehumidifier.

For the hot water cycle, sea water is pumped from the hot water tank to the first solar collector. Then, it is further heated in the second solar collector to reach the design temperature. After that, hot seawater (feed water) is sprayed and cooled down by mixing with the air that flow into the humidifier from the atmosphere using two fans.

As a result of that mixing, some of the feed water is evaporated and carried by air whereas the remaining feed water moves back to the hot water tank to complete the closed loop hot water cycle. It is important to state that the humidifier is arranged to have a cross flow pattern for both water (flowing vertically down on the packing material) and air (flowing horizontally across the humidifier).

Air which leaves the humidifier with high humidity (about 100% relative humidity) flows to the dehumidifier to cool down and condense the water vapor (the product) and exits again to the atmosphere. This air cooled by the water that flows from the cold

water tank to the dehumidifier before it circulated again to the cold water tank to complete cold water the closed loop cycle. The cold water tank is selected to be a huge tank so that its temperature remains almost unaltered.



Figure 9: System photo.

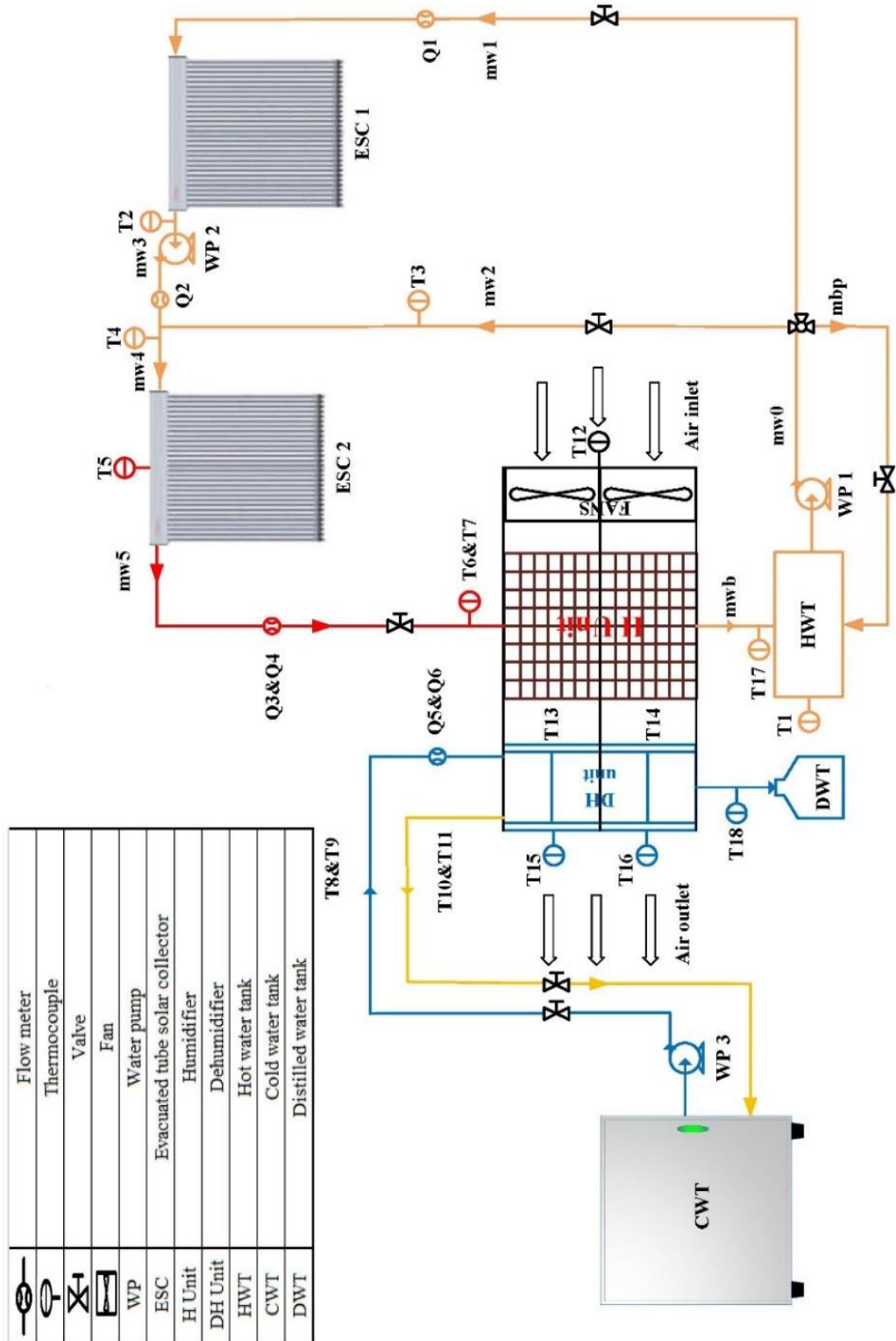


Figure 10: The system under investigation

3.1 System process description

The system is operated in forced convection mode using 3 pumps for the water closed cycles and 2 fans to move the air through the system. Packing materials were used in the humidifier to increase heat and mass exchange surface area resulting in making the humidification process more efficient.

First, seawater in the hot water tank (m_{w0}, T_0) is preheated in the first solar collector (m_{w2}, T_2), then it is further heated in the second solar collector (m_{w5}, T_5). It is then sprayed over the packing material inside the humidifier (m_{w5}, T_7) and leaves as brine at the bottom of the humidifier (m_b, T_{17}) before it recirculated back to the hot water tank (m_{w0}, T_0). The atmosphere air (T_{a1}, ϕ_1) flows by fans to the humidifier to mix with the feed water in a cross-flow arrangement and carries the water vapor (T_{a2}, ϕ_2) before it condenses the water vapor is collected in the dehumidifier bottom (T_a) before air leaves again to the atmosphere (T_{a3}, ϕ_3)

The cold water at the cold water tank ((m_{cw1}, T_8) & (m_{cw2}, T_9)) cools the humid air at the dehumidifier and the temperature of the cold **water increased to** ((m_{cw1}, T_{10}) & (m_{cw2}, T_{11})). Then, it flows back to the cold water tank, which acts as a sink to cool this water stream again to ((m_{cw1}, T_8) & (m_{cw2}, T_9)).

3.2 System components

3.2.1 Humidifier

Basically, it can be considered as a heat exchanger where hot water sprayed to heat and humidity the inlet dry air. The humidifier consists of water spraying mechanism, packing materials (or sometimes called as humidifier because it is the main part in which the humidification process take place), duct and cover.

In the setup, two side by side ducts were manufactured. Each duct made of G.I sheet with thickness 1mm and has a rectangular cross-section with dimensions of 105 x 45 x 40 cm. It is covered by Fiberglass working as an insulation material to prevent system heat losses.

Inside each duct, the water spraying mechanism is positioned at the duct top for effective wetting of the packing. A container with a rectangular cross-section made of Plexiglas with a numerous number of small holes at the base of that container serves as a water spraying mechanism.

The packing material is made of cellulosic-based closed packed evaporating pads. The pads dimensions are 30 x 45 x 40 cm Located at the center of each duct.

Hot water flowing from the solar collectors enters the water spraying container at the top of the humidifier. Then, hot water distributes homogenously wetting the packing materials after it falls down from the container holes. Finally, dry air pushed by fans pass through wetted packing materials from one side, and exits as humid air (after carrying the water vapor, which evaporate due to mixing hot water and air at packing materials surface) at the other side where the dehumidifier is positioned.



Figure 11: System font view.

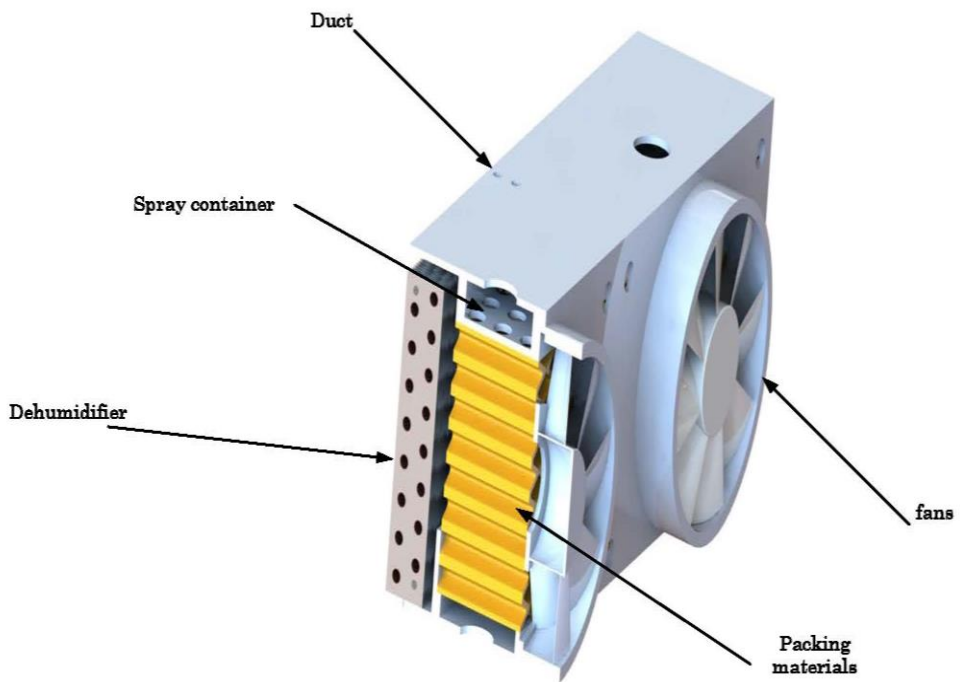


Figure 12: System inside section.

3.2.2 Dehumidifier

The dehumidifier is a device used to condense the water vapor carried by humid air, for that reason finned tube heat exchanger is used to achieve that purpose.

Two identical side by side dehumidifiers are used, one for each duct. The dehumidifier is made from copper (for the tubes) and aluminum (for the fins). The dehumidifier works when the cold water is pumped from the cold water tank to the tubes inside the dehumidifier. On the other hand, humid air passes through the fins side, as result of the temperature difference between the humid air and the cold water, the heat starts to transfer causing water vapor carried by air to condense on the outer surface of the tubes. At last the distilled water is collected at the bottom of the dehumidifier in the distillate water tank.

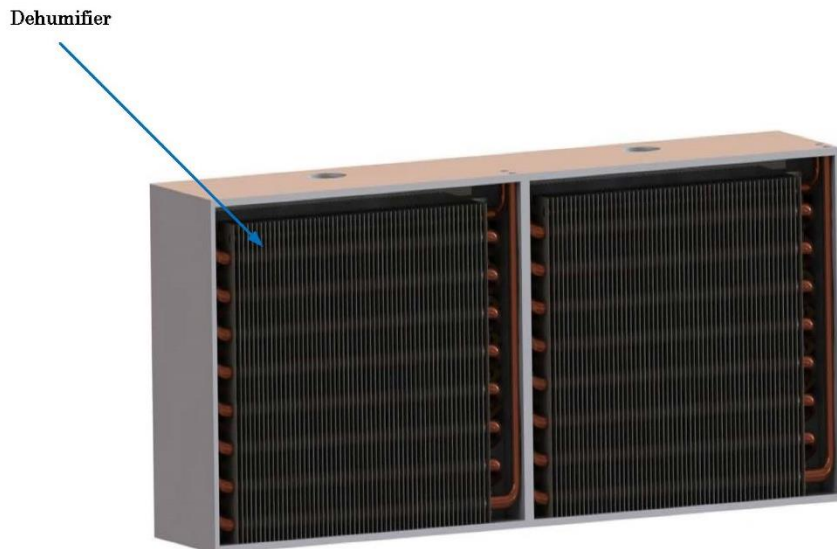


Figure 13: System backside view.

3.2.3 Solar collector

Solar collectors absorb radiation from the sun and transform it to heat via a transfer medium (water). In order to operate the system, two evacuated tube solar collector was putting in series making sure that the system is supplied by hot water.

Evacuated tube solar collector with 180 liters built-in tank and 1.2 m^2 effective area has been selected for their high water temperature generated and high efficacy, especially on a small-scale system.

3.2.4 Auxiliaries

A number of auxiliaries are installed on the system are listed below:

Table 1: Auxiliaries

Component Name	Quantity	Specifications
Fans	2	Maximum Airspeed 0.35 m/s each
Pumps	3	Power 0.5 HP each
Small size hot water Tank	1	50 L capacity
Big size cold water Tank	1	300 L capacity
Variable Transformer	1	Controls the fans speed from 0-0.35 m/s

3.2.5 Measurement Instruments

Many measurement Instruments were needed for testing and controlling the system to show system capability and efficiency such as thermocouples, flow

meters, weather meter, Rotary Thermocouple Selector Switches, data acquisition system reader, hygrometer, graduated cylinder and a stopwatch.

3.2.5.1 Thermocouples

K-type thermocouples are used for measuring the temperature at different system locations. For example, water temperature before and after each system component such as solar collectors, the humidifier and the dehumidifier. Also, air temperature at humidifier inlet and dehumidifier outlet.

3.2.5.2 Panel Mount Flow meter

Panel Mount flow meters are used. They not only can measure the flow rate of water, but also may control the flow rate using a valve emerged at the bottom of the flow meter.

3.2.5.3 Weather meter

Kestrel Meter 4000 Weather Meter handheld is a device used measuring air properties at the humidifier inlet and dehumidifier outlet. Properties such as air speed, humidity, and air temperature are measured.

3.2.5.4 Digital Thermometers

Digital Thermometers Omega HH200A is a reader for converting thermocouple signal to digits on its screen.

3.2.5.5 Rotary Thermocouple Selector Switches

Rotary thermocouple selector switch (Omega SW142-24B) is a manual data acquisition system used as an intermediary device between thermocouples and Digital Thermometers. For a system with numerous number of thermocouples, it is not reliable that each thermocouple has its own reader, for that reason comes the importance of rotary thermocouple selector switches.

At one side there are many pins that it can be connected with thermocouples, each pin defined with a **certain** number (from 1 to 20), also one of the pins specify only to connect the Digital thermometers reader. The other side contain a switcher, therefore when the temperature reading needed for a specific thermocouple in the system, we would only rotate the switch to it is defined number and record **the reading**.

3.3 System Performance Metrics

In HDH system the performance can be described by:

3.3.1 Gain Output Ratio (GOR):

The GOR is the ratio between the latent heat of vaporization of fresh water and the rate of heat consumed to produce it, .i.e. it means the efficiency criterion of the system, which defines the amount of heat recovery.

$$GOR = \frac{m_d * h_{fg}}{Q_{in}} \quad (3.1)$$

3.3.2 Mass Ratio (MR):

The ratio of the mass flow rate of feed water to air mass flow rate.

$$MR = \frac{m_w}{m_a} \quad (3.2)$$

3.3.3 Effectiveness (ε)

Measures the difference between the actual heat of transfer between the water and air to the ideal transfer inside humidifier and dehumidifier.

- For humidifier:

$$\varepsilon_{ha} = \frac{h_{a\ out} - h_{a\ in}}{h_{a\ out\ ideal} - h_{a\ in}} \quad (3.3)$$

$$\varepsilon_{hw} = \frac{h_{w\ in} - h_{w\ out}}{h_{w\ in} - h_{w\ out\ ideal}} \quad (3.4)$$

$$\varepsilon_h = \max \left(\frac{h_{a\ out} - h_{a\ in}}{h_{a\ out\ ideal} - h_{a\ in}}, \frac{h_{w\ in} - h_{w\ out}}{h_{w\ in} - h_{w\ out\ ideal}} \right) \quad (3.5)$$

$h_{a\ out\ ideal}$ The ideal enthalpy of humidifier outlet air can be considered as the enthalpy of the same air with the temperature equal the temperature of hot water entering the humidifier.

$h_{w\ out\ ideal}$ Equal the enthalpy of hot water leaving the humidifier (Brine) if it leaves with a temperature equal the air inlet temperature.

- For the dehumidifier

$$\varepsilon_{dha} = \frac{h_{a\ in} - h_{a\ out}}{h_{a\ in} - h_{a\ out\ ideal}} \quad (3.6)$$

$$\varepsilon_{dhw} = \frac{h_{w\ out} - h_{w\ in}}{h_{w\ out\ ideal} - h_{w\ in}} \quad (3.7)$$

$$\varepsilon_{dh} = \max \left(\frac{h_{a\ in} - h_{a\ out}}{h_{a\ in} - h_{a\ out\ ideal}}, \frac{h_{w\ out} - h_{w\ in}}{h_{w\ out\ ideal} - h_{w\ in}} \right) \quad (3.8)$$

$h_{a\ out\ ideal}$ Equivalent to the enthalpy of air leaving the dehumidifier if it is temperature cooled to the temperature of cold water entering the dehumidifier with the same air humidity.

$h_{w\text{ out ideal}}$ Can be measured as enthalpy of water at inlet air temperature.

3.3.4 Governing equations

For predicting system performance, the governing equations basically are used. They are the mass and energy balance equations for each system components.

3.3.4.1 Humidifier:

Basically we two side by side humidifiers, so the mass and energy equation for the both can be written as follow:

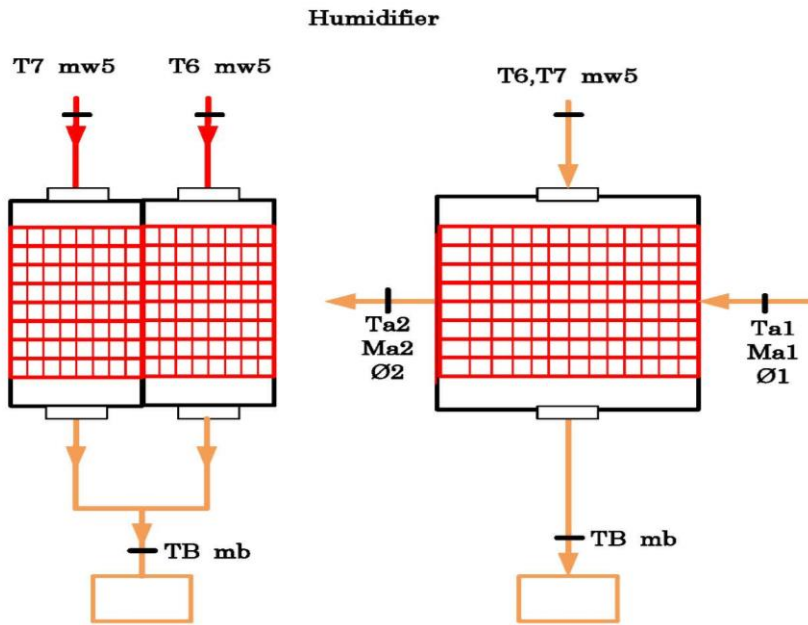


Figure 14: Side and front view of the humidifier.

Mass balance:

$$\dot{m}_{w5} - \dot{m}_b = \dot{m}_{a1} * (\omega_{a2} - \omega_{a1}) \quad (3.9)$$

Energy balance:

$$\dot{m}_{w5} * (h_6 + h_7) - \dot{m}_b * h_b = \dot{m}_{a1} * (h_{a2} - h_{a1}) \quad (3.10)$$

3.3.4.2 Dehumidifier:

Similar to the humidifier, the system contains two dehumidifier used for fresh water production.

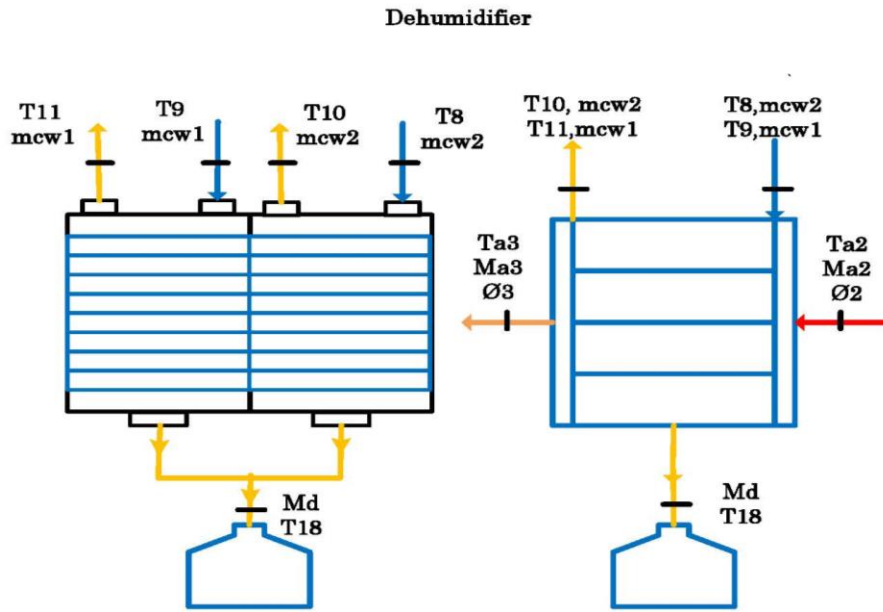


Figure 15: Side and front view of the Dehumidifier.

Mass balance:

$$\dot{m}_d = \dot{m}_{a2} * \omega_{a2} - \dot{m}_{a3} * \omega_{a3} \quad (3.11)$$

Energy balance:

$$(\dot{m}_{cw1} * h_{11} - \dot{m}_{cw1} * h_9) + (\dot{m}_{cw2} * h_{10} - \dot{m}_{cw2} * h_8) + \dot{m}_d * h_{fg} = (\dot{m}_{a3} * h_{a3} - \dot{m}_{a2} * h_{a2}) \quad (3.12)$$

3.3.4.3 Solar collectors:

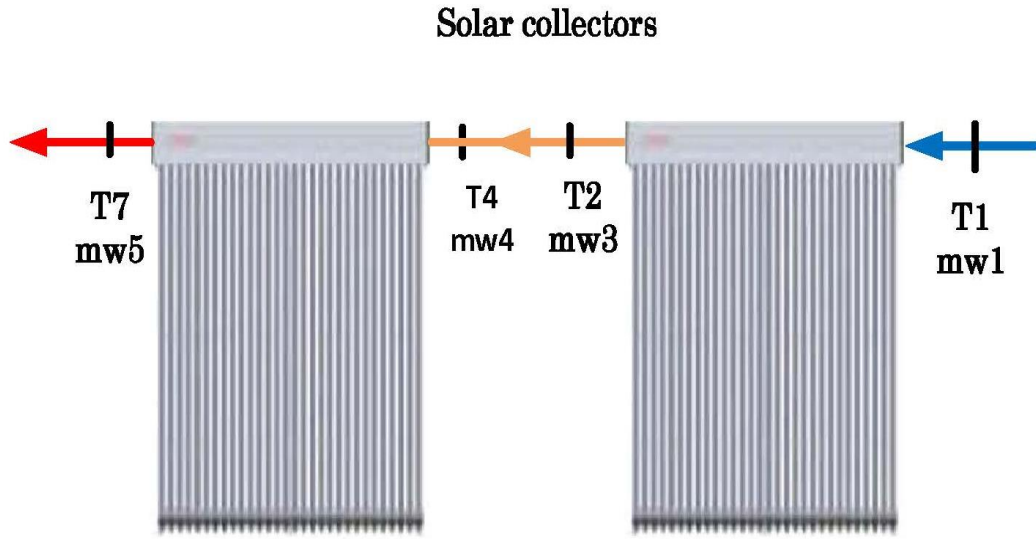


Figure 16: Solar collectors.

Energy balance:

$$Q_{in} = (\dot{m}_{w3} * h_2) - (\dot{m}_{w1} * h_1) + (\dot{m}_{w5} * h_7) - (\dot{m}_{w4} * h_4) \quad (3.13)$$

3.4 System Performance Test

The following steps used to get the Data necessary for system analysis:

1. Make sure that the temperature of the hot water at the second solar collector tank (T5) is more than 60 °C.
2. Open all system valves.
3. Switch on all system pumps and fans.
4. Adjust the flow rate to the selected flow rate value for hot water entering the humidifier and cold water at the dehumidifier.
5. Wait until the system reach the steady operation condition.
6. Make sure that your distilled water tank is empty.

7. Record the initial temperature at each thermocouples.
8. At each selected time intervals take a reading for water temperature at all positions, also record the air temperature, speed and humidity entering and leaving the humidifier and the dehumidifier.

Measuring air properties (Temperature, speed and humidity) at the humidifier inlet requires taking an average value for the air properties at many positions through the duct rectangular cross section at humidifier inlet. This is due to the considerable difference between the properties of air (especially air speed and humidity) at the center of the duct and near duct edge. The same procedure must be followed for the air properties at the dehumidifier outlet.

3.5 Test condition

Due to the water flow rate limitation at the system location, only one side of the system (one humidifier and dehumidifier) was tested to get systems results.

As result of operating only on side of the system, the energy equations for both humidifier and dehumidifier can be rewritten as follow:

$$\dot{m}_{w5} * h_7 - \dot{m}_b * h_b = \dot{m}_{a1} * (h_{a2} - h_{a1}) \quad (3.14)$$

$$(\dot{m}_{cw2} * h_{10} - \dot{m}_{cw2} * h_8) + \dot{m}_d * h_{fg} = (\dot{m}_{a3} * h_{a3} - \dot{m}_{a2} * h_{a2}) \quad (3.15)$$

CHAPTER 4

RESULTS

4.1 Introduction

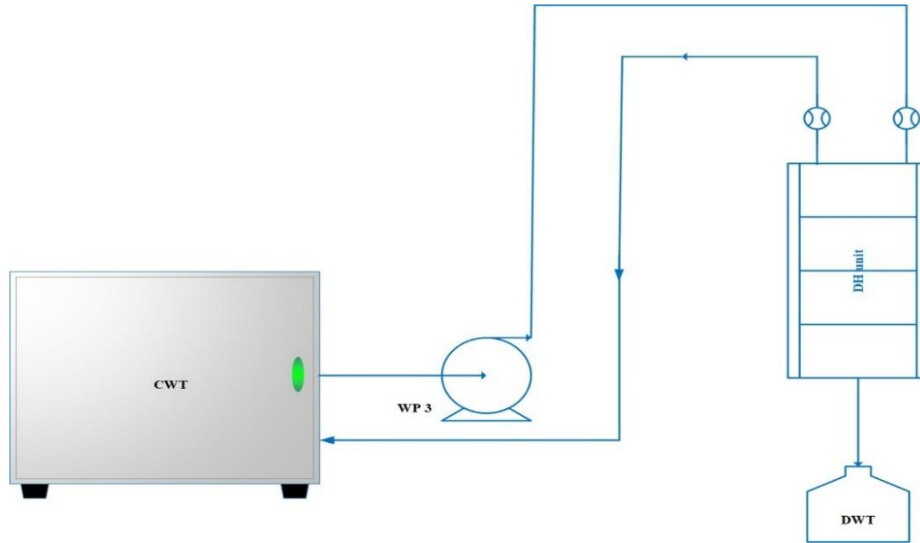
Experimental and Theoretical results of two configurations of the mobile HDH system in which they only differ in the cold water cycle are presented in this chapter. The first configuration has a closed cold water cycle between the dehumidifier and the cold water tank, the second one has an open cold water cycle in which the cold water is disposed after leaving the dehumidifier as shown in [Figure 17](#).

The open cold water cycle HDH system is used during summer. This is because of the cold water high-temperature gain in the dehumidifier, which causes a rise in the temperature of the cold water tank, followed by a reduction in the amount of distilled water, so it is preferred to drain the cold water after leaving the dehumidifier and replaced it with cold water come from any source (for example water tap which used on this experimental).

During winter, the close cold water cycle HDH system can be used, due to the low water temperature at the cold tank and the cold operating conditions, which reduce the effect of temperature gains at the dehumidifier.

At last no cooling device was used for both configuration, only cold water form water tap used as cold water supply for cold water tank.

(a) close cold water cycle



(b) open cold water cycle

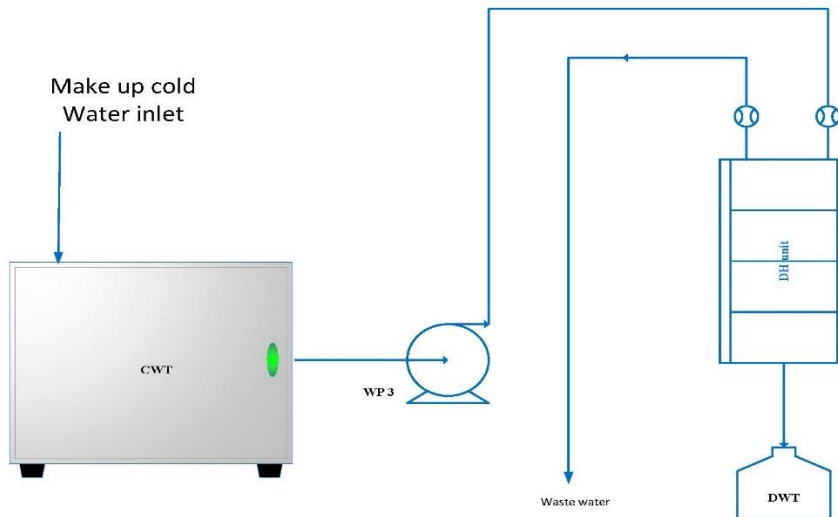


Figure 17: cold water cycles.

4.2 Experimental results

In each configurations, the effect of many parameters on both system production (\dot{m}_d) and performance (GOR) are reported such as:

- The effect of top cycle temperature (T_7).
- The effect of air flow rate (\dot{m}_a).
- The effect liquid to air mass flow rate ratio (MR) by:
 - Changing air flow rate (\dot{m}_a).
 - Changing hot water flow rate (\dot{m}_w).

As results of water flow rate limitation at the system location, only one side of the system (one humidifier and dehumidifier) was tested to get these results. (The systems contains two side by side humidifier and dehumidifier as shown on the figure below [figure 18](#)).

4.3 Open cold water cycle mobile HDH system

The system contains two water cycles, a hot water cycle between the humidifier and the solar collectors and a cold water cycle between the cold water tank and the dehumidifier. For the hot water cycle, sea water is pumped from the hot water tank to the first solar collector. Then, it is further heated in the second solar collector to reach the design temperature. After that, hot sea water (feed water) is sprayed and cooled down by mixing with the air that flow into the humidifier from the atmosphere using two fans. As result of that mixing, some of the feed water is evaporated and carried by air whereas the remaining feed water move back to hot water tank to complete the closed loop hot water cycle. The air which leaves the humidifier with high humidity (about 100% relative humidity) flows to the dehumidifier to cool down and condense the water vapor (the product) and exits

again to the atmosphere. This air cooled by water that flows from the cold water tank to the dehumidifier before it rejected to the surrounding, a makeup cold water coming from water tap replaces the amount of cold water rejected. **Figure 18**

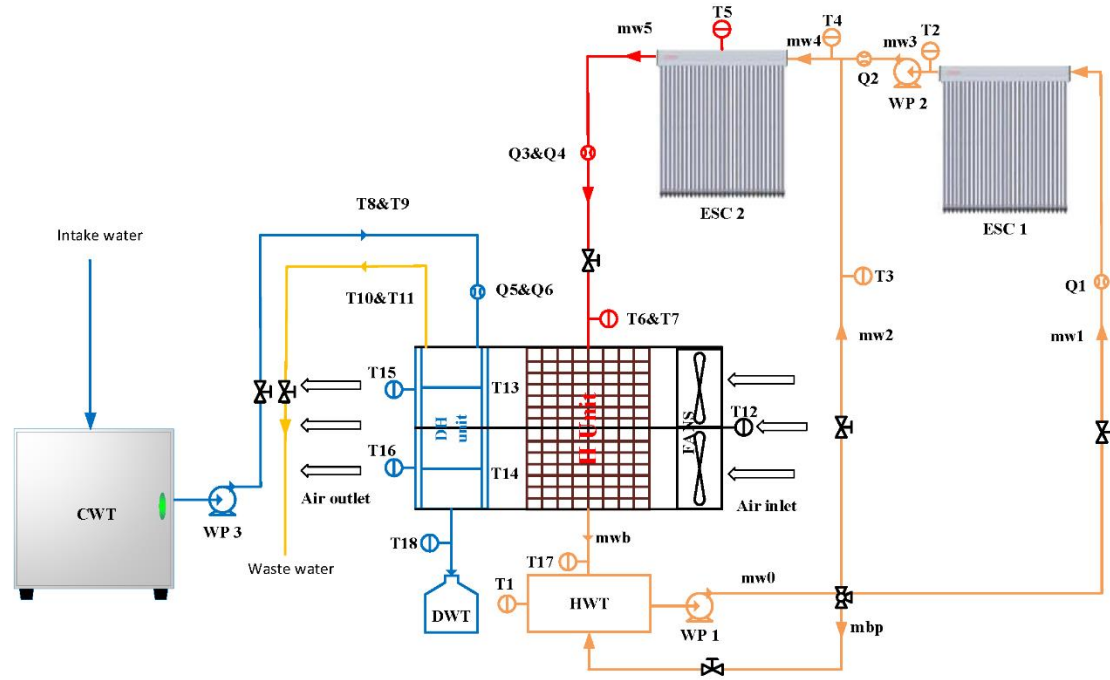


Figure 18: Open cold water cycle mobile HDH system.

4.3.1 The effect of top cycle temperature at the humidifier inlet (T7)

Figure 19 Shows the effect of changing the humidifier inlet temperature (Top cycle temperature T7) at different water flow rates (3,4and 5 LPM) on the system performance. The experiment demonstrates that increasing the top cycle temperature T7 results in increasing both GOR and system production (m_d), since the ability of absorption of water

vapor by air increased with the rise in temperature at the humidifier which directly affect the humidification and condensation process in both humidifier and dehumidifier.

So, by air increased with the rise in temperature at the humidifier which directly affect the humidification and condensation process in both humidifier and dehumidifier.

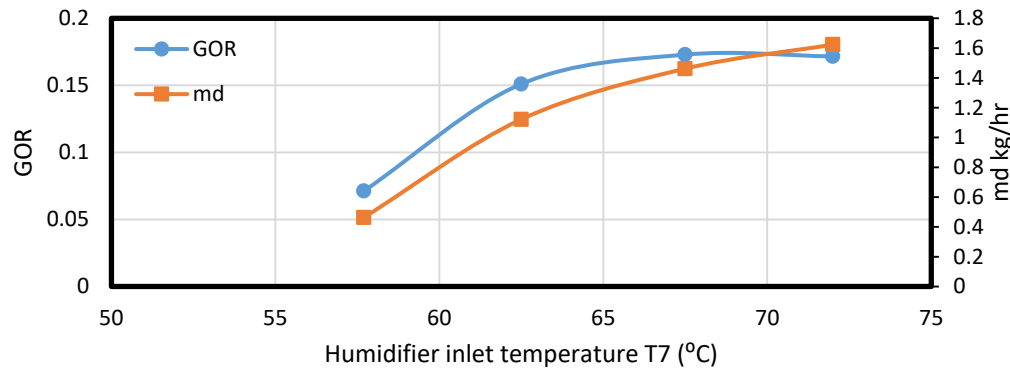
So, for operation; condition are almost constant for different flow rates, with 35 °C and 30% relative humidity for the inlet air in addition to having a temperature of 33 °C for cold water temperature. At 3 LPM (180 kg/hr) seawater flow rate at the humidifier, the GOR rises slightly from 0.15 to 0.25 when the top cycle temperature increases from 55 to 70 °C. Meanwhile, fresh water production improves more than 100% (0.75 to 2 kg/hr) when the temperature increases by the same range.

For a humidifier water flow rate of 4 LPM (216 kg/hr), there is a significant increase for both GOR and the fresh water production (from 0.15 to 0.3 and from 1 to 4 kg/hr for system GOR and production, respectively).

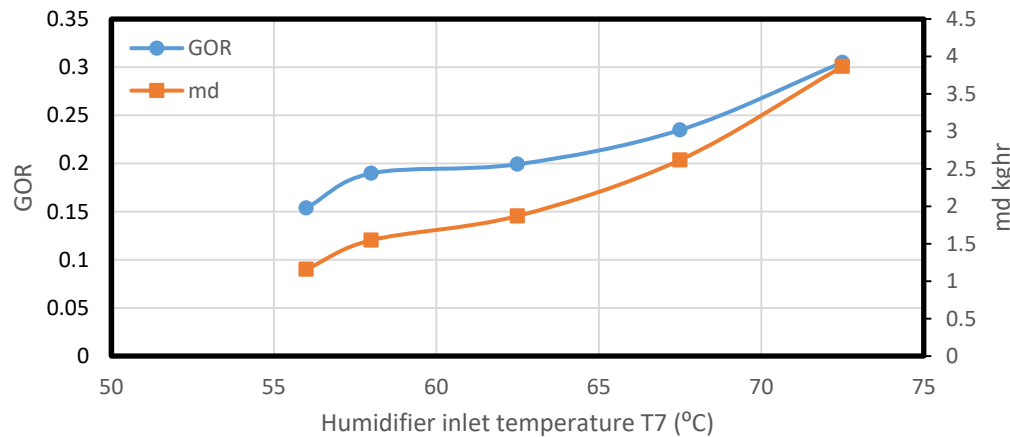
Moreover, the system shows the same trend of the effect of temperature effect at 5 LPM (252 kg/hr) humidifier water flow rate, with GOR of 0.35 and 4.5 kg/hr distilled water production at 72.5 °C and drops to (0.22 and 2.5 kg/hr) when the humidifier top temperature decreases to 62.5 °C.

From all figures below, it can be noticed that at low humidifier top temperature, increasing the water flow rate has a small effect on both system performance and production. In contrast at high humidifier top temperature, there is a huge improvement in the system performance as we increase the humidifier water flow rate.

(a) Q= 3 LPM



(b) Q = 4 LPM



(C) Q= 5 LPM

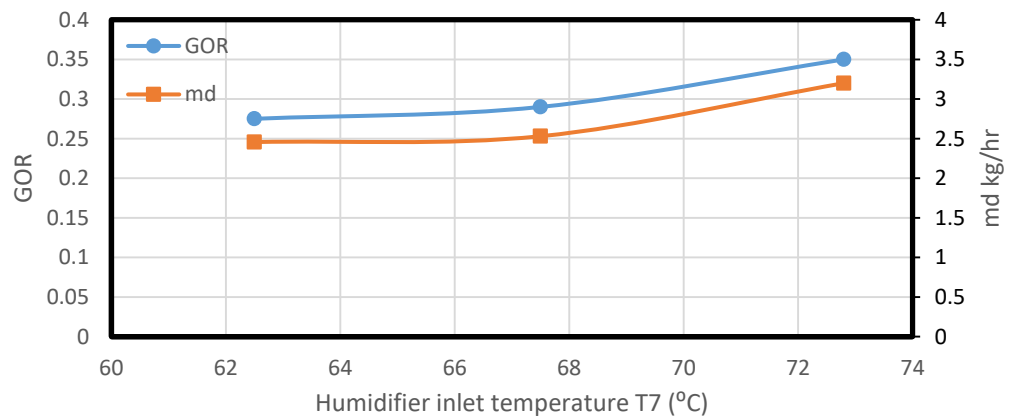
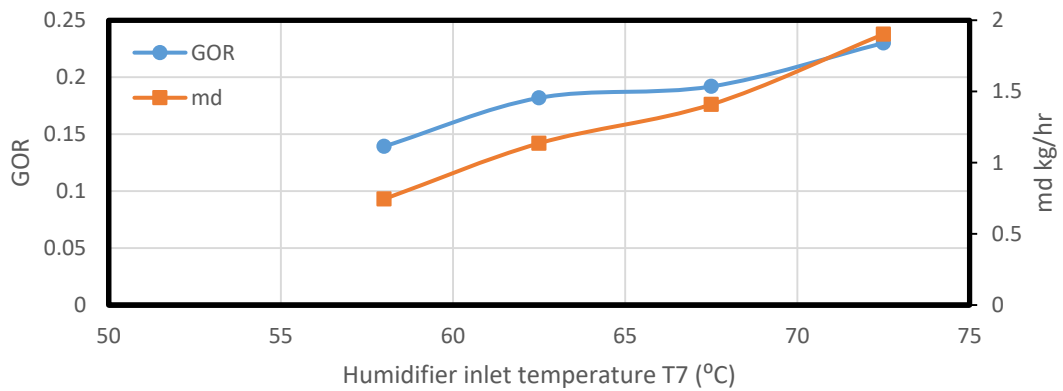
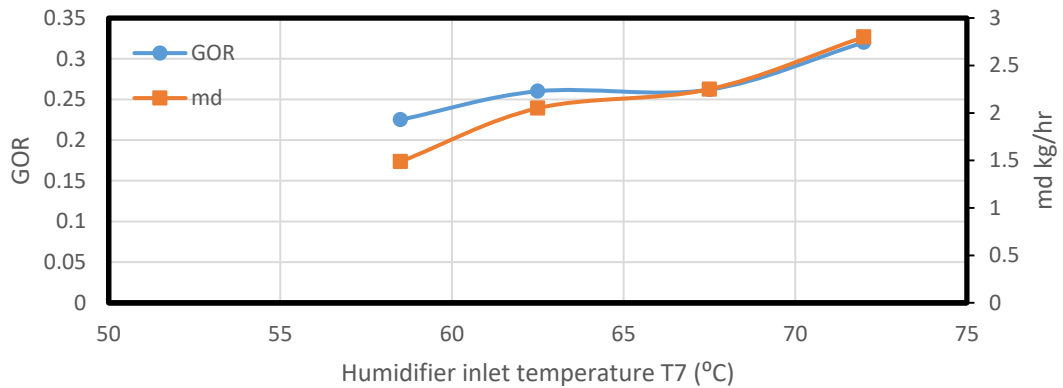


Figure 19: The effect of top cycle temperature at $\dot{m}_a = 0.075 \text{ kg/s}$ on system performance.

(a) $Q = 3 \text{ LPM}$



(b) $Q = 4 \text{ LPM}$



(C) $Q = 5 \text{ LPM}$

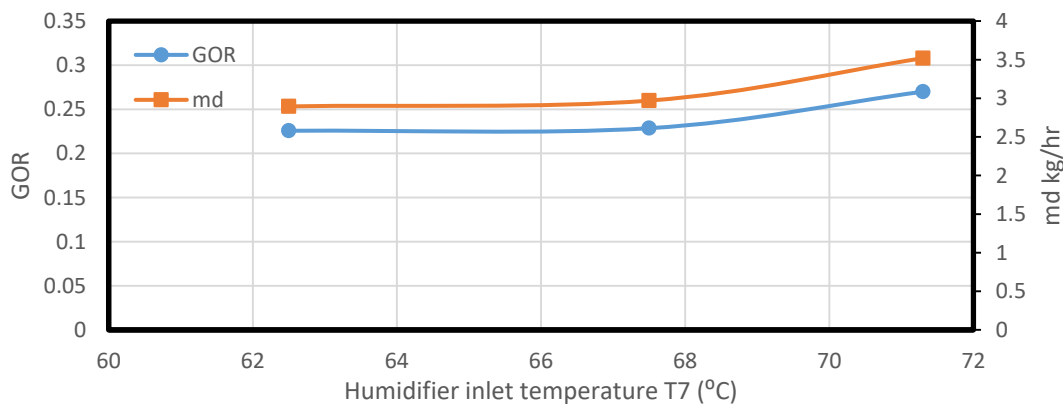


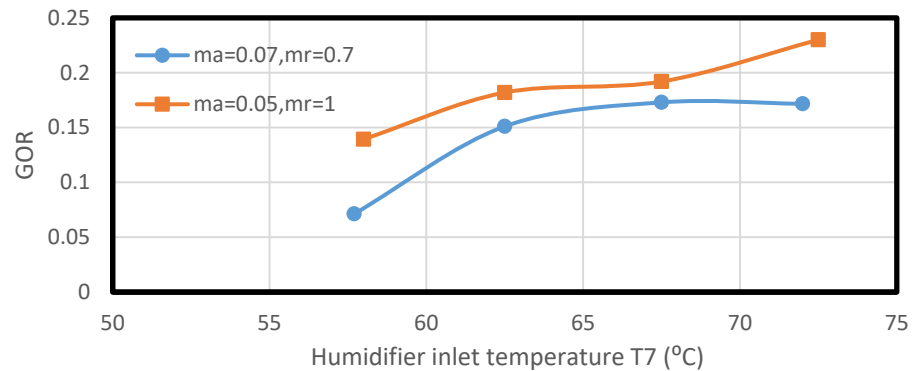
Figure 20: The effect of top cycle temperature at $\dot{m}_a = 0.09 \text{ kg/s}$ on system performance.

4.3.2 The effect of Air flow rate (\dot{m}_a)

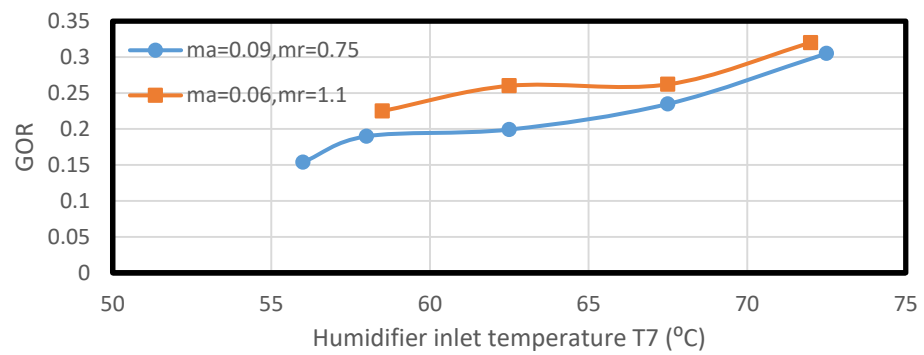
The effect of air flow rate presented by testing the system at two different value of air flow rate using a Variac to control system fans, at different humidifier flow rates (3, 4 and 5 LPM).

From the figures, it observed that the system GOR drops with increasing in the amount of air flow rates. In contrast, the amount of fresh water production increases with growth in air flow rates especially at the top high temperature at humidifier inlet, because increasing the amount of air flow rate means rise in the amount of water vapour needed to humidify the dry air which leads to higher energy consumption at the humidifier. So for that reason, the GOR value reduces and the amount of water production increase associated with the growth of mount water vapor at humidifier carried by air. At humidifier feed water flow equal 3, 4 and 5 LPM, the system tested with two air flow rates at the same operating conditions approximately as shown in [figures 21 and 22](#). The experimental results present that the GOR and the system productivity behavior for all humidifier flow rates have the same trends. GOR values almost double at high temperature with the decrease of the air flow rate (e.g. 0.175 & 0.2 GOR rise to 0.25 & 0.325 for humidifier water flow rate equal 3 and 5, respectively at top temperature equal 72.5 °C when then the air flow rates increase by 0.02 Kg/s). Furthermore, changing air flow rate affects the system productivity at high temperature (At 72.5 °C, the freshwater amount reduce from 4 & 3.5 kg/hr to 2.5 & 3 kg/hr for humidifier water flow rates of 4 and 5 LPM). At lower temperatures, there is no considerable change with varying air flow rate.

a) $Q = 3 \text{ LPM}$



b) $Q = 4 \text{ LPM}$



c) $Q = 5 \text{ LPM}$

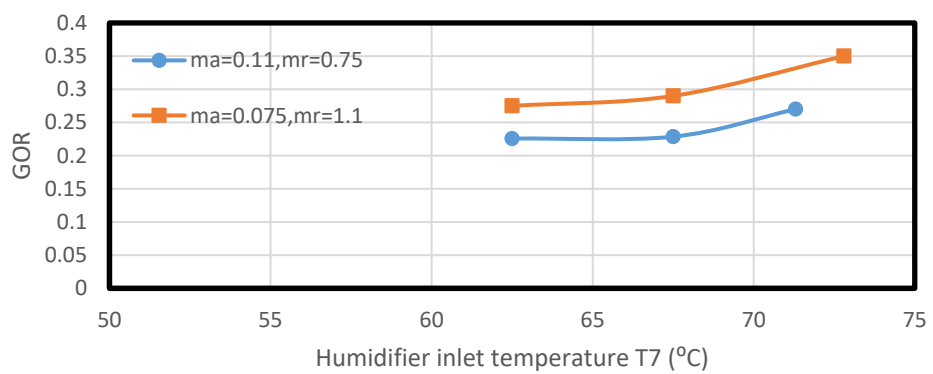
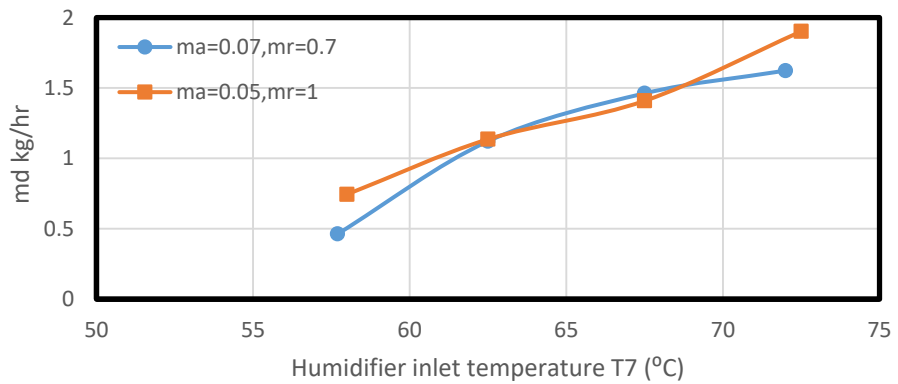
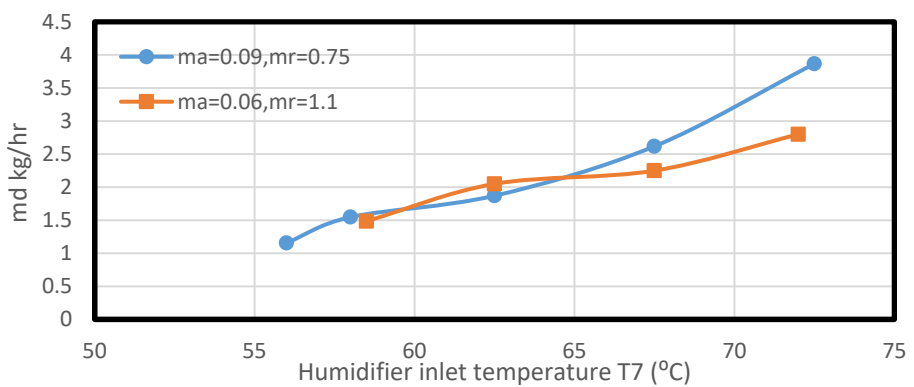


Figure 21: The effect of Air flow rate \dot{m}_a on system GOR.

a) **$Q = 3 \text{ LPM}$**



b) **$Q = 4 \text{ LPM}$**



c) **$Q = 5 \text{ LPM}$**

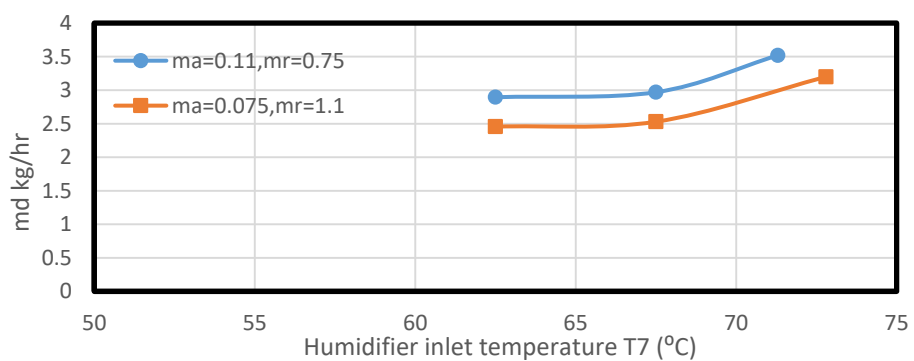


Figure 22: The effect of Air flow rate \dot{m}_a on fresh water production.

4.3.3 The effect of liquid to Air flow rate ratio (MR)

There are two ways that can be used in order to present the effect of liquid to air mass ratio on system performance, either changing air flow rate while keeping water flow at a fixed value or changing water flow rate with a fixed air flow rate.

4.3.3.1 by changing air flow rate (\dot{m}_a)

Increasing the water to air mass ratio (through varying air flow rate) dropped system GOR at all used humidifier water flow rates tested (3,4 and 5 LPM). This is expected due to the increase in power needed to meet the increase of water vapor amount required. [Figure 21](#)

The figure also shows that at lower air flow rate (almost equal to 0.06 kg/s) for all humidifier flow rates, the system GOR grows with humidifier water temperature rise until it reaches a certain value (corresponding to 60 C in this case). Then, the GOR remains almost constant for a temperature range between 60 C and 65 C. After that range of temperature, the GOR rises again with humidifier temperature (above 65 C). At high air flow system GOR increases with humidifier temperature monotonically over the used range of temperature.

In contrast with the experimental data, the fresh water production increases with the increase in mass flow rat ratio (air flow rate) at high humidifier temperature. However, at low temperature, the experimental results show that there is a small change in system production (md) as the effect of altering water mass flow rate ratio as presented in [figure 4.22.](#)

4.3.3.2 by changing water flow rate (m_w)

In case of changing water to air mass flow rate ratio by varying humidifier water flow rate, a decline of the water to air mass ratio results in dropping of both systems GOR and freshwater production, which means while we increased the amount of mass ratio MR we move forward to optimum mass ratio which gives best system performance. The optimum mass ratio guarantees that the right amount of water vapour sprayed at the humidifier, so more than that amount of water vapour will not increase the humidity of air, on the other hand less than that amount of water vapor leads to nearly dry air leaves the humidifier. On this system the optimum mass ratio cannot be reached due to the experiment limitation (fans speed which control the amount of air flow rates), but the only things that sure, it happens at mass ratio higher than 1.1 (the highest possible mass ratio using fans maximum speed).

This was tested at three different humidifier flow rates (3, 4 and 5 LPM). Each of these results is presented at two air flows rate (0.8 and 0.6 kg/s). [Figures 23, 24.](#)

- **At $ma=0.08 \text{ kg/s}$ at the humidifier.**

From [figure 4.23](#) at a humidifier inlet water temperature equal to 60 C, system GOR and production was 0.15 and 1 kg/hr. at 0.62 air-water mass ratio, then it rises to 0.2 & 0.27 GOR and 2 & 2.5 kg/hr fresh water when the mass ratio increase to 0.75 & 1.1 at the same humidifier temperature. After that at high-temperature system performance was 0.15 & 0.3 & 0.35 GOR and 2 & 2.6& 3.5 kg/hr of fresh water production for 0.62, 0.75 & 1.1 air-water mass ratio respectively.

- **At $ma=0.06$ kg/s at the humidifier.**

Following the same procedure as before, two different mass ratio (0.8 and 1.1) was tested at 0.6 kg/s air flow rate.

It was noticed that both GOR and fresh water production almost double with a growth of air-water mass ratio, so for the GOR it improve from 0.13 & 0.24 at 57 & 72.5 °C humidifier temperature and 0.66 mass ratio, to 0.24 & 0.34 for the same temperature and 0.88 mass ratio. As for the freshwater production, it follows the trends of system GOR, so it enhances from 0.75 & 2 kg/hr at 0.66 mass ratio, to 1.5 & 3 kg/hr at 0.88 mass ratio.

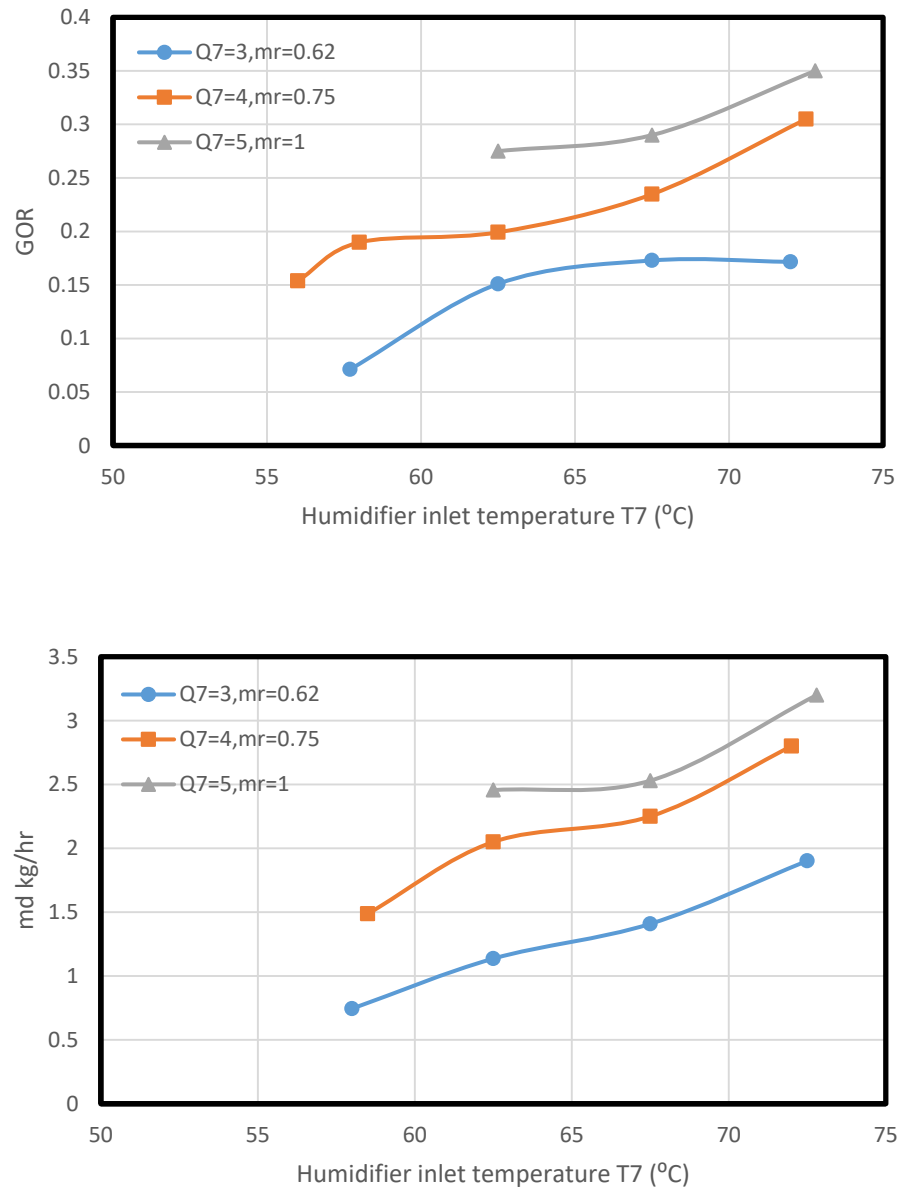


Figure 23: The effect of mass ratio on system performance MR at $\dot{m}_a = 0.08 \text{ kg/s}$.

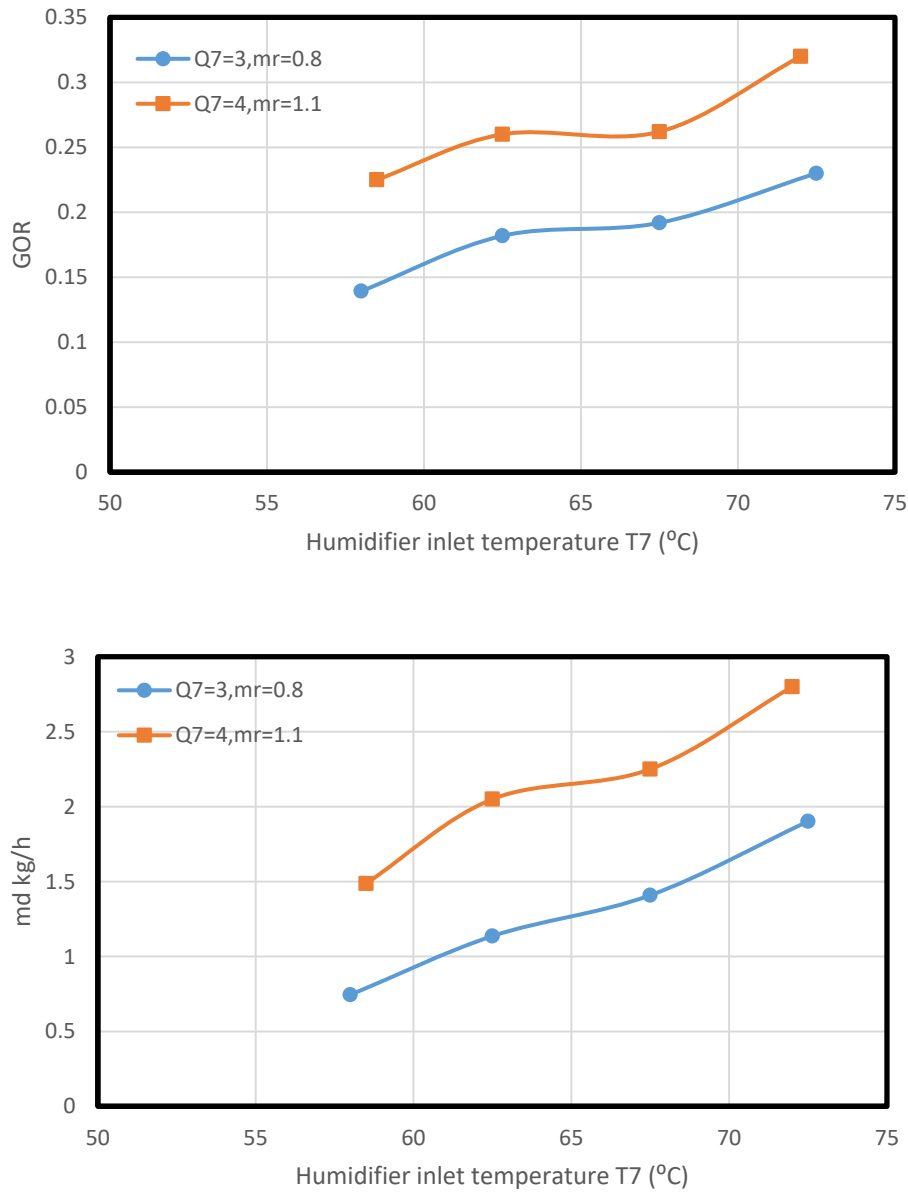


Figure 24: The effect of mass ratio MR on system freshwater production at $\dot{m}_a = 0.06$ kg/s.

4.4 Close cold water cycle mobile HDH system

The close cold water cycle HDH system works almost identical to the open cold water cycle HDH system, the only difference exist at the cold water cycle, so instead of rejected the cold water which used to cool down the humid air at the dehumidifier, it circulated again to the cold water tank to complete cold water closed loop cycle. The cold water tank is selected to be a huge tank so that its temperature remain almost unaltered.

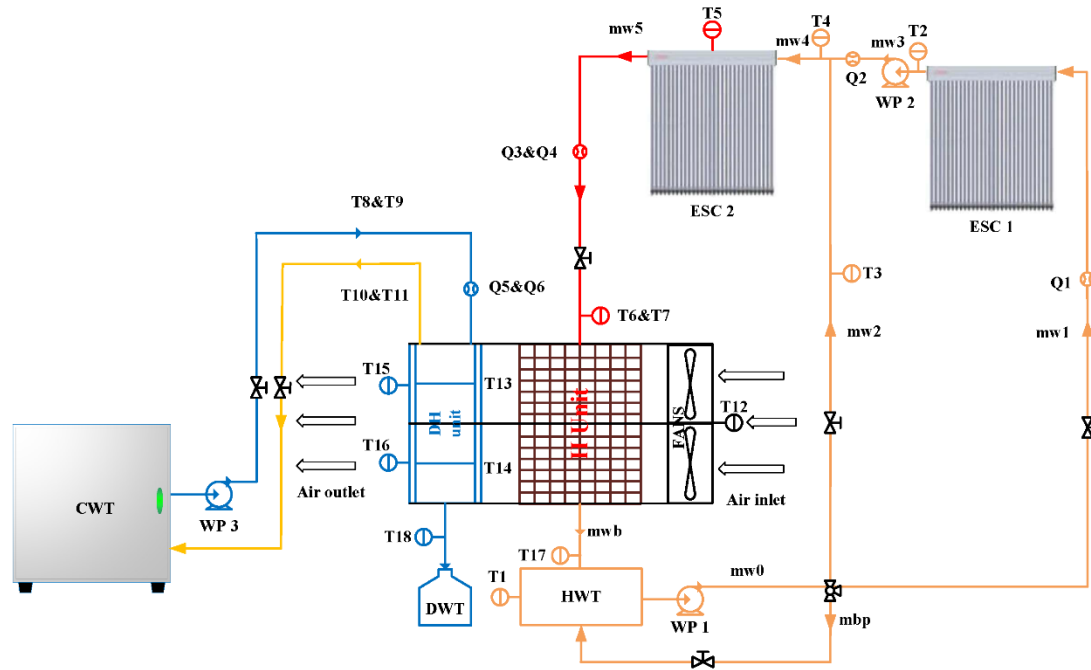


Figure 25: Close cold water cycle mobile HDH system.

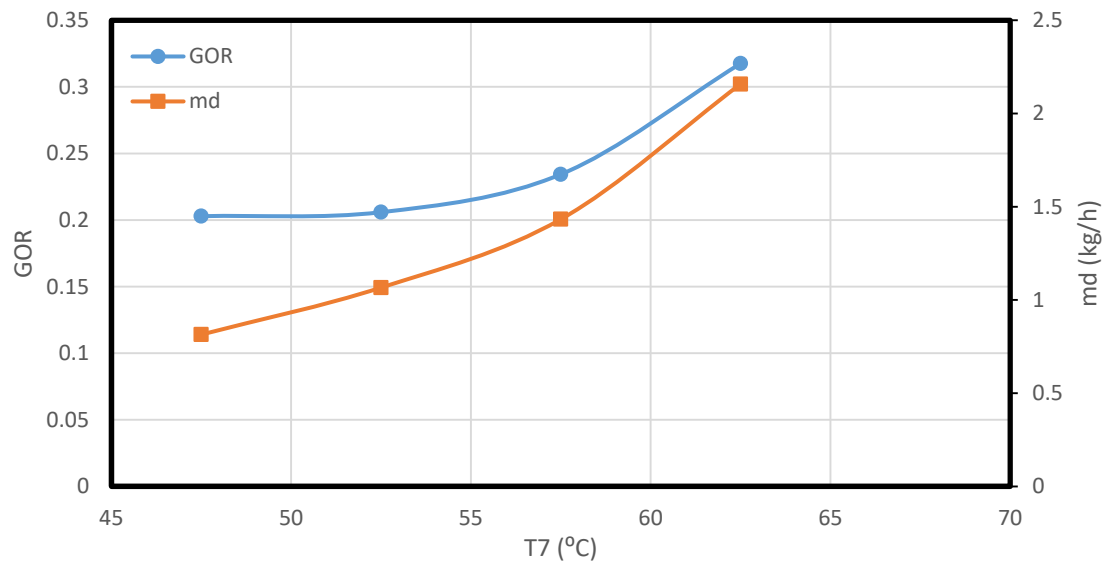
4.4.1 The effect of top cycle temperature (T7)

As shown from figures below ([figures 26 and 27](#)), both system GOR and production increase with the rise in inlet humidifier water temperature, this behaviour change at high temperature (above 60°C) in which the growth in GOR and fresh water production become more sharply. Rising humidifier top temperature increase the humidifier effectiveness

(humidification process) which leads that the air leaves the humidifier with high humidity that directly increase the distilled water production at the dehumidifier (condensation process). For all cases, GOR starts almost about 0.2 at low temperature and exceeds 0.3 at high temperature. Also, the range of fresh water production is about 1 kg/hr and 2.5 kg/hr at low and high temperatures, respectively, except at the case when the air flow rate is 0.048 kg/s and humidifier water flow rate equal to 0.06 kg/s. This case provides a water product between 2 and 5 kg/hr, which the highest freshwater production recorded during system testing.

Lastly it is noticed that the GOR and water production values remains constant at low top humidifier temperature range which indicate that the dehumidifier reached maximum capacity associated with the cold water temperature used to cool down the humid air.

a) Q= 3 LPM



b) Q = 4 LPM

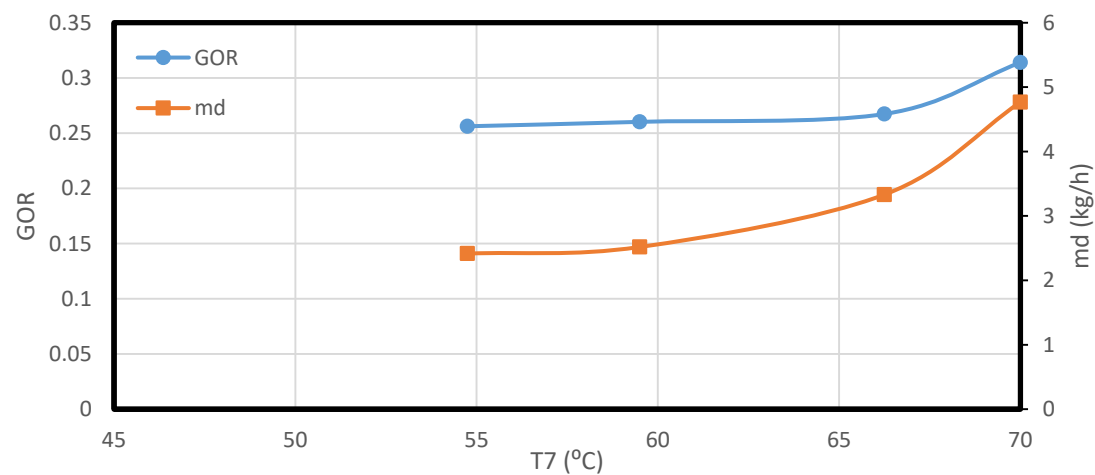
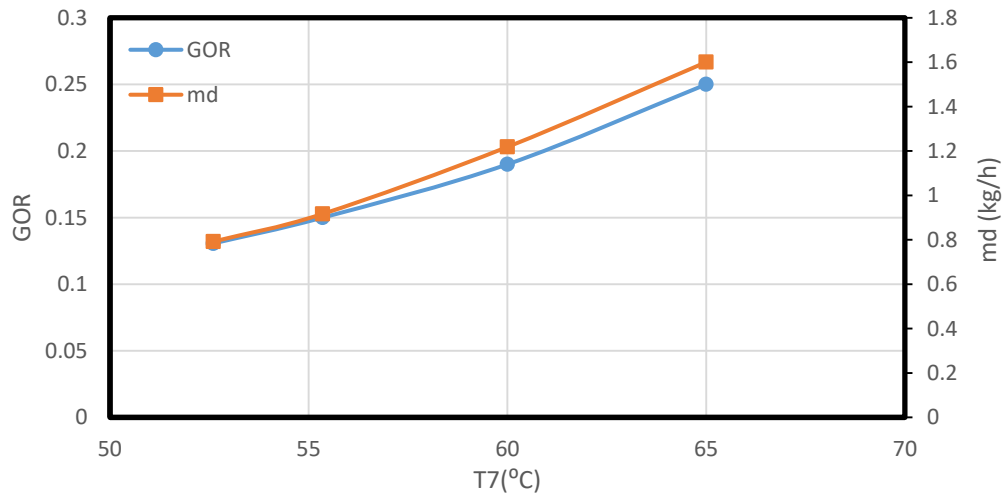


Figure 26: The effect of top cycle temperature T7 at $\dot{m}_a = 0.048 \text{ kg/s}$ on GOR.

a) Q= 3 LPM



b) Q = 4 LPM

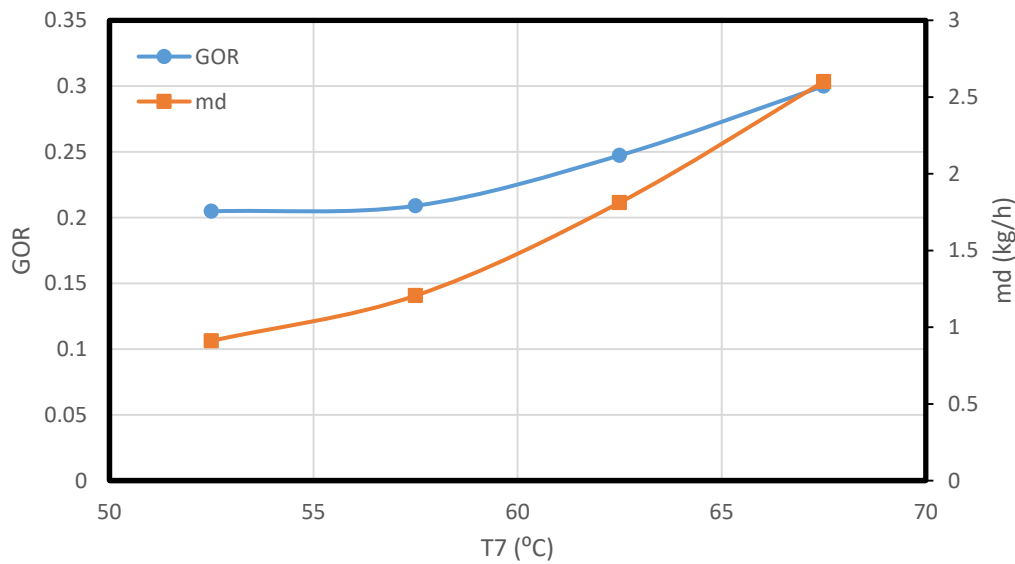


Figure 27: The effect of top cycle temperature T7 at $\dot{m}_a = 0.03 \text{ kg/s}$ on GOR.

4.4.2 The effect liquid to Air flow rate ratio (MR)

4.4.2.1 by changing water flow rate

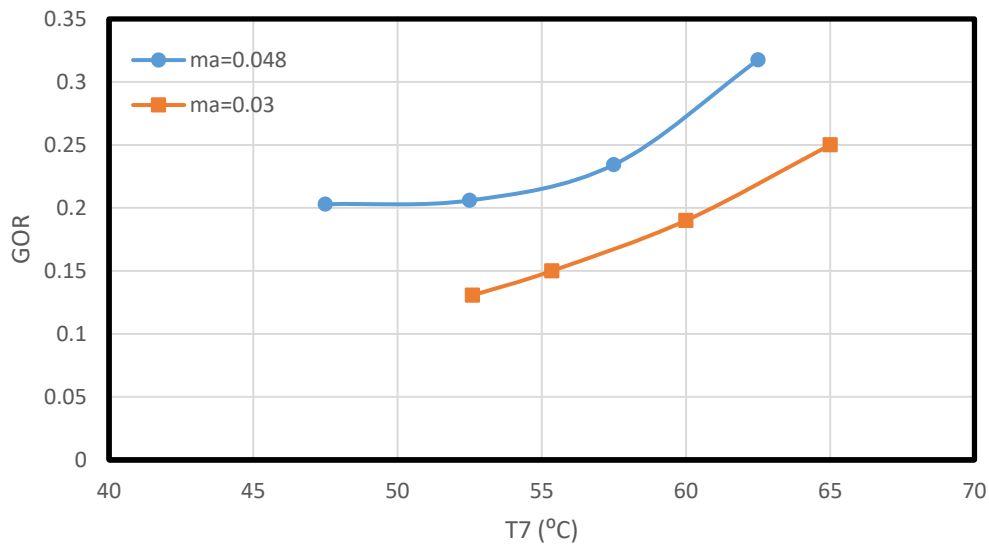
Unlike the close cold water HDH system in which, increasing the amount of inlet air at the humidifier reduce system GOR. Here, with this type of configuration, the growth in air flow rate is associated with improving the GOR of the system.

The reason of that in the case is that the dehumidifier effectiveness rises up with air flow rate. It is important to state that the cold weather has a considerable impact on the dehumidifier effectiveness associated with the air flow rate, which in some cases results in a dehumidifier effectiveness that approaches 100 %. This results in an increase in the amount of distilled water, which make a huge jump on the value of the GOR compared with the reduction on GOR related to the growth in input energy required with the increase in the air flow rate.

From [figure 28](#) the GOR rises from 0.15 to 0.2 when the air flow rate increases by 0.01 kg/s at 50 °C humidifier temperature and 0.05 Kg/s water humidifier flow rate, also for the same operating condition but at higher humidifier temperature (65 °C) the GOR increase from 0.2 to 0.35. The same behaviour happened at 0.06 Kg/s humidifier water rate, in which the GOR growth from 0.2 to 0.25 at 50 °C humidifier temperature, as well increase from 0.3 to 0.33 at 65 °C humidifier temperature at the same working condition.

In contrast, the fresh water production almost doubles with the increase in air flow rate such that the growth from 1 and 2.5 kg/hr to 2 and 4.9 kg/hr at 50 and 70 °C humidifier inlet water temperature and 0.06 kg/s humidifier water flow rate as shown in [Figure 29](#).

a) $Q = 3 \text{ LPM}$



b) $Q = 4 \text{ LPM}$

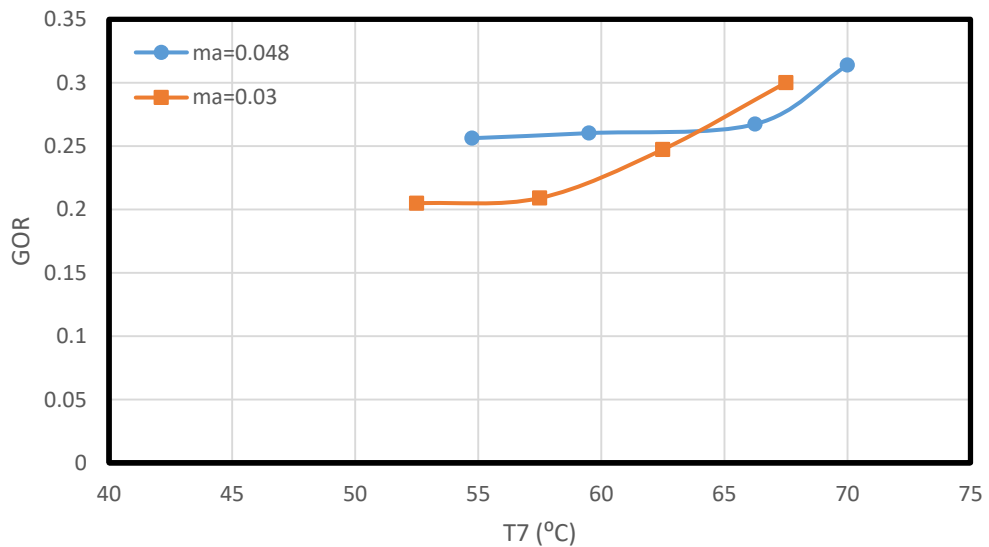
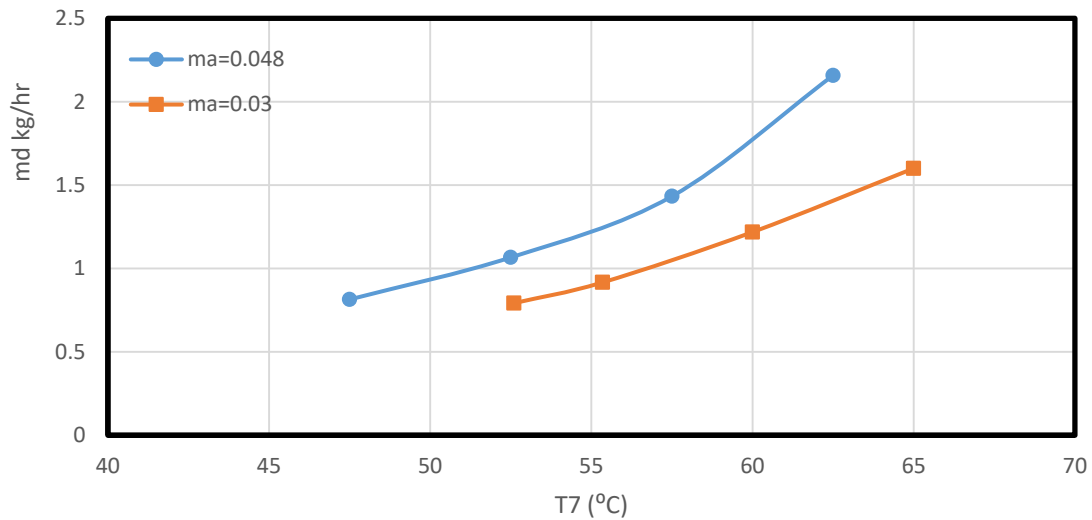


Figure 28: The effect of Air flow rate \dot{m}_a on system GOR.

a) $Q = 3 \text{ LPM}$



b) $Q = 4 \text{ LPM}$

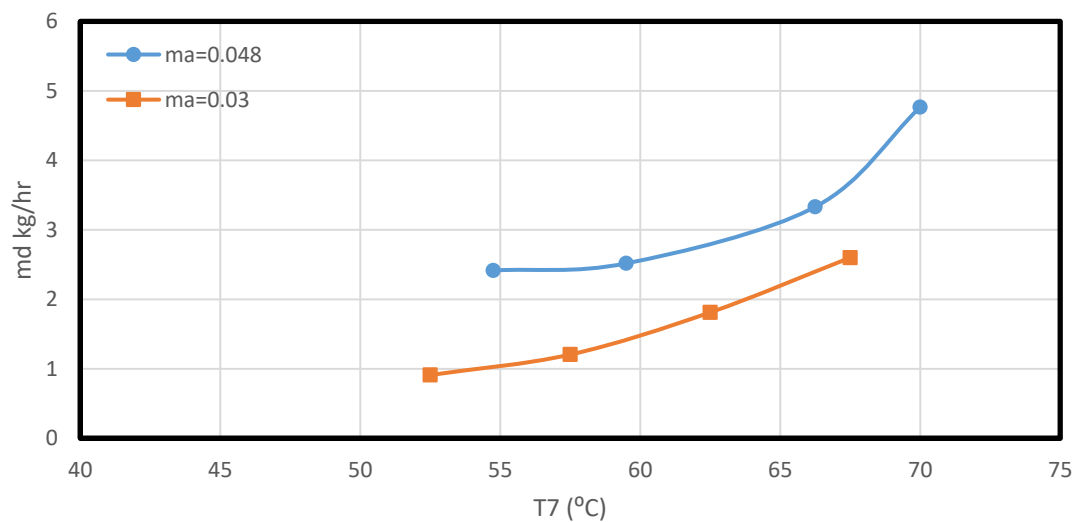


Figure 29: The effect of Air flow rate m_a on freshwater production m_d .

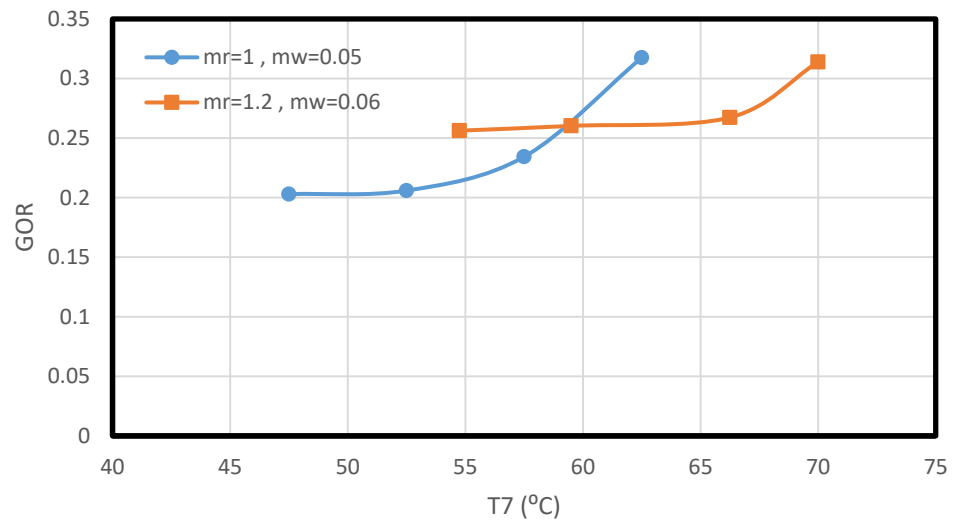
4.4.2.2by changing water flow rate

Although there is a slight effect on system GOR by changing water to air mass ratio at high humidifier temperature (above 60 °C). However, at low top cycle temperature (below 55 °C) there is a considerable change by altering the mass ratio as shown in [figure 30](#). That is because increasing the amount of the feed hot water at the humidifier rise the quantity of water vapor generated, and thus growth the amount of fresh water condensate at the dehumidifier which increase the values of both GOR and distilled water production. At air flow rate equal 0.048 Kg/s at humidifier inlet, the system GOR almost equals 0.27 for mass flow rate ratio values of 1 and 1.2, respectively. Furthermore, for the same operating condition but different humidifier temperature range (below 55 °C), the GOR equals 0.2 and 0.15 for mass flow rate ratios of 0.6 and 0.5. The same effect of changing mass ratio on GOR is also exhibited at 0.03 kg/s humidifier water flow rate, with 0.15 and 0.1 system GOR for 0.6 and 0.5 mass ratios at top cycle water temperature of 55 °C at the inlet of the humidifier, and almost equal 0.2 for both mass ratios at 65 °C.

Increasing the mass ratio reduces the fresh water production as presented in [figure 31](#). For example for humidifier inlet water temperature of 60 °C, distilled water production drops from 2.5 to 1.5 kg/hr at an air flow rate of 0.048 kg/s when the air-water ratio increase from 1 to 1.2.

The same happens in a similar operating condition at 0.03 kg/s air flow rate when the mass ratio increases from 0.5 to 0.6, we find that the freshwater production reduce by 1 kg/hr.

a) $m_w = 0.05 \text{ kg/s}$



b) $m_w = 0.06 \text{ kg/s}$

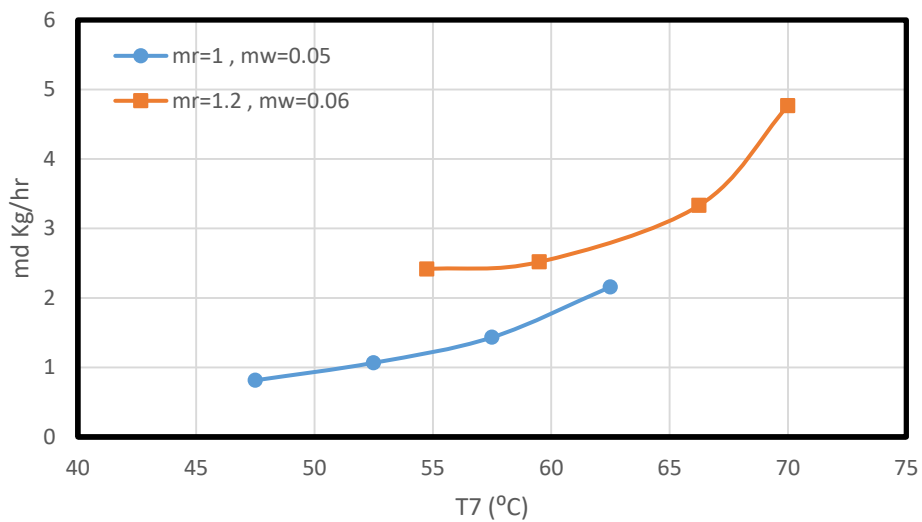
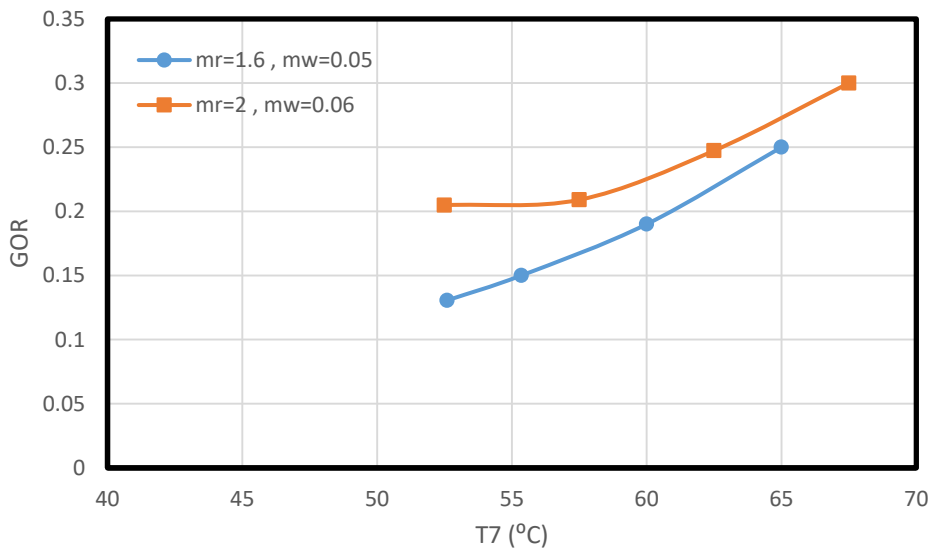


Figure 30: The effect of mass ratio MR on system performance at $\dot{m}_a = 0.048 \text{ kg/s}$.

a) mw = 0.03 kg/s



b) mw = 0.06 kg/s

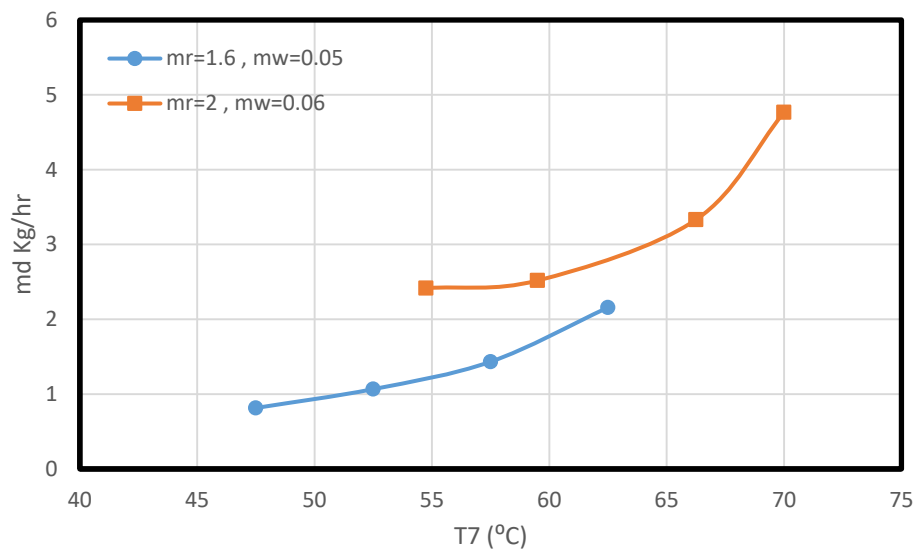


Figure 31: The effect of mass ratio MR on system performance.

4.5 Experimental and Theoretical results comparison

Theoretical analysis was done for both configurations of HDH mobile system to see the difference between the theoretical results based on the mass and energy equations for each device on the system and the experimental results. Another benefit of the theoretical analysis is the ability to predict the system results at conditions that cannot be achieved experimentally.

Using similar operating condition for both theoretical and experimental analysis for the two HDH system configurations shows that, although the theoretical and experimental results have a huge difference in its values but, it almost follow the same lines trends for both GOR and fresh water production, as shown in [figure 32](#) and [figure 33](#).

[Figures 32](#) and [figure 33](#) shows a sample of results compares the experimental and theoretical analysis for both configurations, for example, the open cold water cycle HDH system at high humidifier top temperature (70°C) and 4 LPM hot water flow rate shows 0.88 GOR theoretically which almost double the experimental result (0.41 GOR). Both the theoretical and experimental results drop as the humidifier top temperatures decrease (i.e 0.75 and 0.28 on the theoretical and experimental analysis at 60°C humidifier top temperature).

Meanwhile for fresh water production rise with the increase in top humidifier temperature reaching about 10 Kg/hr theoretically at 70°C , which almost triple the experimental value (3 Kg/hr).

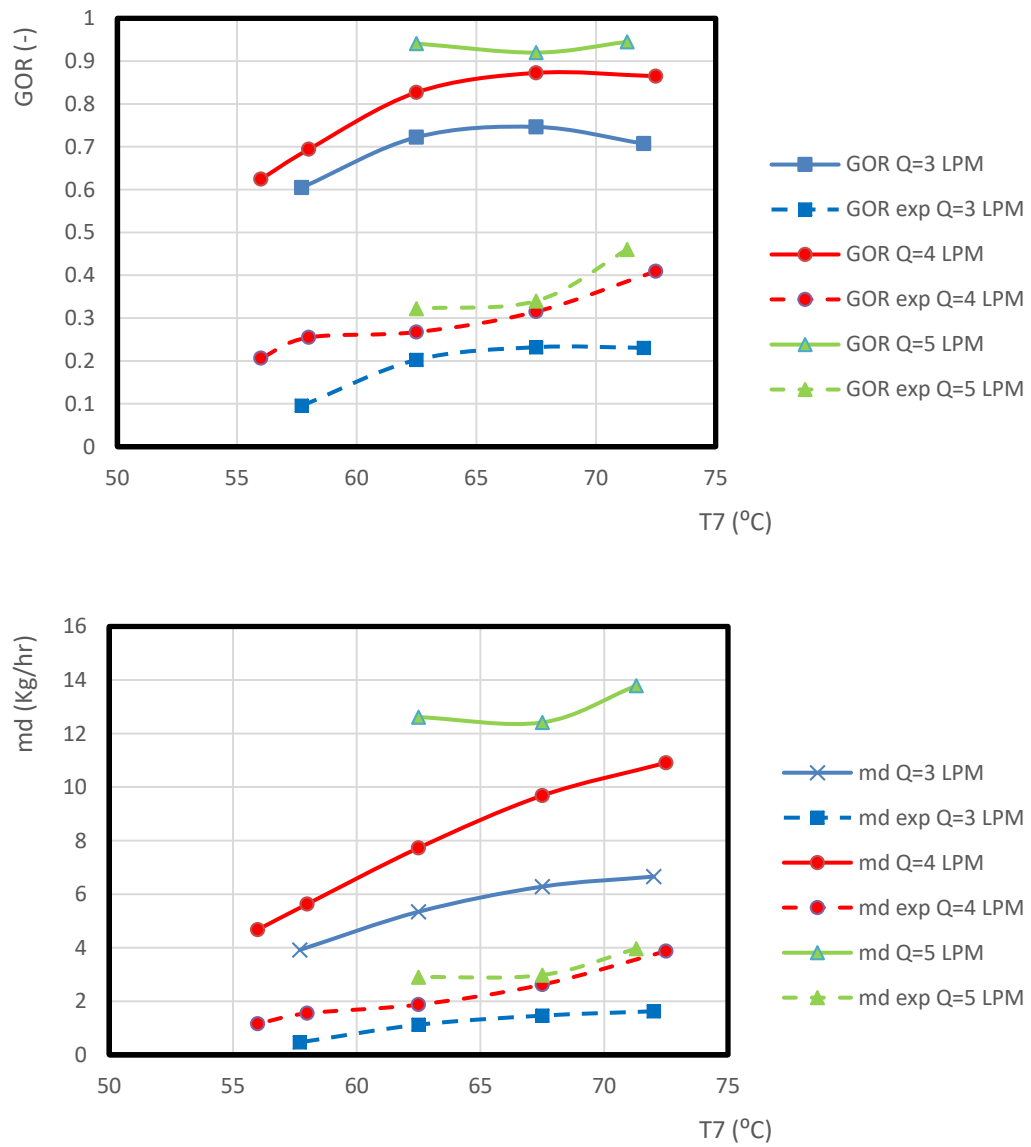


Figure 32: Theoretical and experimental results for the open cold water cycle HDH system.

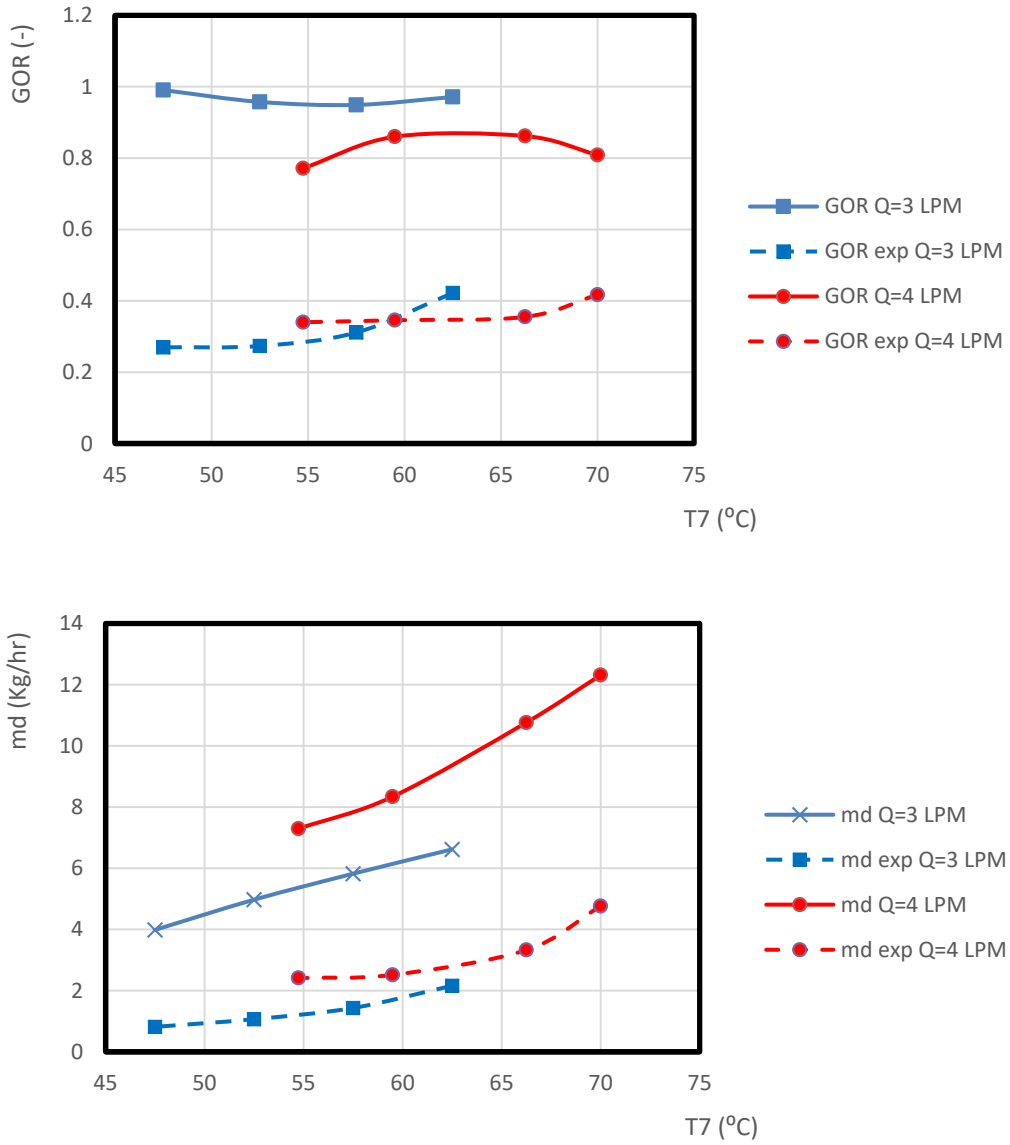


Figure 33: Theoretical and experimental results for the close cold water cycle HDH system.

CHAPTER 5

CONCLUSIONS & RECOMMENDATIONS

5.1 CONCLUSIONS

An investigation of the performance of two configurations of a mobile HDH system was carried out experimentally. The system set-up is modified and connected with manual data acquisition system to record the data coming from the thermocouples which measure the temperature of air and water after and before each device made up the system (humidifier, dehumidifier, solar collectors and etc...). The effects of changing the main parameters on the system performance (GOR and fresh water production) are analyzed, and finally, a brief comparison between the experimental and theoretical results are presented.

The setup was tested with the operating condition as follows, a hot feed water flow rates between 3 and 5 LPM at the humidifier, hot water with maximum temperature up to (70 °C) at some cases, dehumidifier cold water flow rates equal 7 LPM and maximum water – air mass ratio less than 2.

The experimental results for the open and close cold water HDH system shows that:

- For the open cold water cycle mobile HDH system, the maximum GOR tested experimentally was 0.35 at the humidifier water flow rate equal to 5 LPM and 1.1 water-to-air mass flow rate ratio (MR), and the maximum fresh water produced was 3.8 Kg/h at humidifier water flow rate equal to 4 LPM and 0.66 water-to-air mass flow rate ratio (MR).
- For the close cold water cycle mobile HDH system, the maximum fresh water produced recorded was 4.7 Kg/h at the humidifier water flow rate equal to 4 LPM

and 1.2 water-to-air mass flow rate ratio (MR), and the maximum GOR was 0.32 at humidifier water flow rate equal to 3 LPM and 0.77 water-to-air mass flow rate ratio (MR).

Based on the experimental study of the two configurations of the HDH system, many of observations can be reached and summarized as follows:

- The system GOR and water production grow with the increase in top hot water feed temperature at the humidifier which appears more clearly at low air flow rate. The reason of that because the high water temperature affect the air by increasing the ability of air to absorb more water vapor associated with the rise in the amount of water vapor generated which means enhance the humidifier performance, also a high water temperature at the humidifier leads to humid air with high temperature leaving the humidifier and entering the dehumidifier, so the huge difference in temperature between the humid air and the cold water at the dehumidifier (high-temperature difference in which the amount of heat can transfer more easily between the hot and the cold side inside the heat exchanger) result in more distilled water production and also affect the GOR.
- The rise in the amount of air flow rate affects the two configurations differently. At the start for the open cold water cycle HDH system, the rise in air flow rate influence both the GOR and the fresh water production in a separate way, by drops the system GOR values and rise the amount of freshwater production. In contrast for a closed water cycle HDH system, the increase in the air flow rate will result in a rise in both the GOR and freshwater production. The reason of that, in the open cold water HDH system, the growth in the amount of air flow leads to increase in

the amount of energy consumption at the humidifier to maintain the operation running (increase the air flow rate means, growth in the amount of water vapour needed to humidify the air entering the humidifier which leads to higher energy consumption). So the value of the GOR drops as the effect of energy required but in a different way the fresh water production growth as a result of increasing the amount of humid air entering the dehumidifier. For the close cold water cycle HDH systems, the rise in airflow effects the distilled water production the same way as the open cold water cycle, but in the other side the GOR growth with an air flow rate which is different. The reason of that as it mention before in chapter 4, that the close cold water cycle design for winter season, and the open for the summer, so during winter due to low operating temperature which leads to higher dehumidifier effectiveness (as shown at appendix A), and as a result of that increase in the freshwater production numbers, this growth has a higher effect in system GOR value than the rise the energy required.

- Both system GOR and fresh water production rise with the increase in water-air mass ratio for both system configurations. This mass ratio MR depends on the ability of air to carry water vapor, so higher the mass ratio number means a higher probability of air to leaves the humidifier as saturated air (100 % relative humidity), which affect directly in improving both The humidifier and the dehumidifier effectiveness, so develop system performance.
- The highest water air mass ratio can be tested by changing fans speeds (control airspeed) and using flow meters (control water flow rate) in the experiment is 2. So maybe at high water air mass ratio, the hot water may produce a higher amount of

water vapor than the amount that can be carried by air, if that happens it will lead to a high drops in the GOR value (unnecessary energy consumption).

The comparison between the theoretical and the experimental analysis shows that although the theoretical and the experimental results have a huge difference in its values but, it almost follows the same effect (the lines trends for both GOR and fresh water production) associated with changing system parameters.

5.2 RECOMMENDATIONS

As the experimental result shows that the system has low performance (maximum GOR Value equal 0.4), most of the recommendation focus on how to modify the system and introduce new modification that can be tested in future work.

- One of the drawbacks of this system that the humidifier has a larger size than the size of the dehumidifier, so the amount of humid air entering the dehumidifier is bigger than the amount that the dehumidifier can handle (this can be noticed if you put your hand at the dehumidifier exit when the system operating, the water vapor condense on your hand, this means the water vapor amount larger than the capacity that can be handled by the dehumidifier), therefore for HDH water heated system the dehumidifier size should be at least double the size of the humidifier.
- In order to make it possible to run the system at a higher water flow rate ((higher than 5 LPM) and run the setup for a longer time, the hot tank size (50 Liters capacity) should be increased to prevent the water flooding at both the humidifier and the hot tank. Sometimes this problem happened even at low flow rate after

operating the system for a time longer than 90 minutes, so it forced to discharge part of the water inside the hot tank which affects system performance.

- Add one more tank to the system set up to store the cold water after leaving the dehumidifier instead of through it away at the drainage, so it can use to fill the solar collectors rather than use the tap water (cold water source), which reduce the amount of time needed to heat the water. Also, this tank can be considered another solution to flooding problem at the hot tank and the humidifier in case it not possible to have a bigger hot tank, so the extra water discharge (usually has a temperature equal 40 °C or higher) to the new tank to use it again later.
- For more accurate results the system setup should put inside close location except the solar parts, so it can be possible to control the operating condition (air temperature and humidity).

References

- [1] M. Zamen *et al.*, “Experimental investigation of a two-stage solar humidification – dehumidification desalination process,” vol. 332, pp. 1–6, 2014.
- [2] O. Barron, E. Campos-pozuelo, and C. Fernandez, “Desalination Technologies: Are They Economical for Urban Areas?,” pp. 341–354, 2016.
- [3] G. P. Narayan, M. H. Sharqawy, E. K. Summers, J. H. Lienhard, S. M. Zubair, and M. A. Antar, “The potential of solar-driven humidification-dehumidification desalination for small-scale decentralized water production,” *Renewable and Sustainable Energy Reviews*, vol. 14, no. 4, pp. 1187–1201, 2010.
- [4] H. E. S. Fath4b and A. Ghazy, “Solar desalination using humidification-dehumidification technology,” *Desalin. ELSEVIER Desalin.*, vol. 142, pp. 119–133, 2002.
- [5] S. A-hallaj, M. Mehdi, and A. Rahman, “Solar desalination with a humidification–dehumidification cycle : performance of the unit,” vol. 120, pp. 273–280, 1998.
- [6] E. Chafik, “A new seawater desalination process using solar energy,” vol. 153, pp. 25–37, 2002.
- [7] M. Farid and F. Hamad, “Performance of a single-basin solar still,” vol. 3, no. 1, 1993.
- [8] M. Engelhardt and W. Sch, “Small-scale thermal seawater desalination simulation and optimization of system design,” vol. 122, pp. 255–262, 1999.
- [9] W. F. He, D. Han, W. P. Zhu, and C. Ji, “Thermo-economic analysis of a water-heated humidification- dehumidification desalination system with waste heat recovery,” vol. 160, no. 29, pp. 182–190, 2018.
- [10] S. M. Soufari, M. Zamen, and M. Amidpour, “Experimental validation of an optimized solar humidification-dehumidification desalination unit,” *Desalin. Water Treat.*, vol. 6, no. 1–3, pp. 244–251, Jun. 2009.
- [11] G. Yuan and H. Zhang, “Mathematical modeling of a closed circulation solar desalination unit with humidification-dehumidification,” *Desalination*, vol. 205, no. 1–3, pp. 156–162, 2007.
- [12] K. Zhani and H. Ben Bacha, “Experimental investigation of a new solar desalination prototype using the humidification dehumidification principle,” vol. 35, no. October 1993, pp. 2610–2617, 2010.
- [13] A. S. Nafey, “Solar desalination using humidification – dehumidification Part II . An experimental investigation,” vol. 45, pp. 1263–1277, 2004.

- [14] B. Bacha, “Modelling and simulation of a water desalination station with solar multiple condensation evaporation cycle technique,” pp. 238–254.
- [15] H. P. Garga, R. S. Adhikarib, and R. Kumarb, “Experimental design and computer simulation of multi-effect humidification (MEH) -dehumidification solar distillation,” vol. 153, 2002.
- [16] C. Yamal, “Theoretical investigation of a humidification- dehumidification desalination system configured by a double-pass flat plate solar air heater,” vol. 205, no. May 2006, pp. 163–177, 2007.
- [17] J. Orfi, N. Galanis, and M. Laplante, “Air humidification – dehumidification for a water desalination system using solar energy,” vol. 203, no. May 2006, pp. 471–481, 2007.
- [18] A. S. Nafey, “Solar desalination using humidification dehumidification processes . Part I . A numerical investigation,” vol. 45, pp. 1243–1261, 2004.
- [19] S. Energy, “Experimental investigation of a solar desalination unit with humidification and dehumidification,” vol. 130, pp. 169–175, 2000.
- [20] A. M. Abdel Dayem, “Efficient Solar Desalination System Using Humidification/Dehumidification Process,” *J. Sol. Energy Eng.*, vol. 136, no. 4, pp. 41014–41019, Jun. 2014.
- [21] G. Al-enezi and H. Ettouney, “Low temperature humidification dehumidification desalination process,” vol. 47, pp. 470–484, 2006.
- [22] X. Li, G. Yuan, Z. Wang, H. Li, and Z. Xu, “Experimental study on a humidi fi cation and dehumidi fi cation desalination system of solar air heater with evacuated tubes,” *DES*, vol. 351, pp. 1–8, 2014.
- [23] G. Yuan, Z. Wang, H. Li, and X. Li, “Experimental study of a solar desalination system based on humidi fi cation – dehumidi fi cation process,” vol. 277, pp. 92–98, 2011.
- [24] A. M. I. Mohamed and N. A. El-Minshawy, “Theoretical investigation of solar humidification-dehumidification desalination system using parabolic trough concentrators,” *Energy Convers. Manag.*, vol. 52, no. 10, pp. 3112–3119, 2011.
- [25] E. Vier, I. S. Bourounia, M. T. Chaibib, and L. Tadrist, “DESALINATION Water desalination by humidification and dehumidification of air : state of the art,” vol. 137, pp. 167–176, 2001.
- [26] Y. Ghalavand, M. S. Hatamipour, and A. Rahimi, “Humidification compression desalination,” *Desalination*, vol. 341, no. 1, pp. 120–125, 2014.
- [27] A. M. I. Mohamed and N. A. S. El-Minshawy, “Humidification-dehumidification desalination system driven by geothermal energy,” *Desalination*, vol. 249, no. 2, pp. 602–608, 2009.

- [28] M. Vlachogiannis, V. Bontozoglou, C. Georgalas, and G. Litinas, “Desalination by mechanical compression of humid air,” vol. 122, pp. 35–42, 1999.
- [29] G. P. Narayan *et al.*, “Status of humidification dehumidification desalination technology,” *World Congr. Conv. Exhib. Cent.*, p. 20, 2011.
- [30] D. Lawal, M. Antar, A. Khalifa, S. Zubair, and F. Al-Sulaiman, “Humidification-dehumidification desalination system operated by a heat pump,” *Energy Convers. Manag.*, vol. 161, no. January, pp. 128–140, 2018.
- [31] M. B. Shafii, H. Jafargholi, and M. Faegh, “Experimental investigation of heat recovery in a humidification-dehumidification desalination system via a heat pump,” *Desalination*, vol. 437, no. November 2017, pp. 81–88, 2018.
- [32] W. F. He, D. Han, and C. Ji, “Investigation on humidification dehumidification desalination system coupled with heat pump,” *Desalination*, vol. 436, no. 29, pp. 152–160, 2018.
- [33] H. Li, Y. Li, Y. Dai, I. Godinez, and R. Wang, “Experimental investigation on a solar assisted heat pump in-store drying system,” *Appl. Therm. Eng.*, vol. 437, no. March, pp. 89–99, 2011.
- [34] A. Giwa, H. Fath, and S. W. Hasan, “Humidification-dehumidification desalination process driven by photovoltaic thermal energy recovery (PV-HDH) for small-scale sustainable water and power production,” *Desalination*, vol. 377, pp. 163–171, 2016.
- [35] G. P. Narayan, R. K. McGovern, S. M. Zubair, and J. H. Lienhard, “High-temperature-steam-driven, varied-pressure, humidification-dehumidification system coupled with reverse osmosis for energy-efficient seawater desalination,” *Energy*, vol. 37, no. 1, pp. 482–493, 2012.
- [36] G. Franchini, A. Perdichizzi, and A. Picinardi, “HD desalination by heat rejected from solar cooling systems,” in *2010 IEEE International Energy Conference*, 2010, pp. 63–68.
- [37] M. Khedr, “Techno-Economic investigation of an air humidification-dehumidification desalination process,” *Chem. Eng. Technol.*, vol. 16, no. 4, pp. 270–274, 1993.
- [38] M. I. Zubair, F. A. Al-Sulaiman, M. A. Antar, S. A. Al-Dini, and N. I. Ibrahim, “Performance and cost assessment of solar driven humidification dehumidification desalination system,” *Energy Convers. Manag.*, vol. 132, pp. 28–39, 2017.
- [39] K. Bourouni, R. Martin, L. Tadrist, and M. T. Chaibi, “Heat transfer and evaporation in geothermal desalination units,” vol. 64, pp. 129–147, 1999.
- [40] C. Muthusamy and K. Srithar, “Energy and exergy analysis for a humidification-dehumidification desalination system integrated with multiple inserts,” *Desalination*, vol. 367, pp. 49–59, 2015.

- [41] M. H. Sharqawy, M. A. Antar, S. M. Zubair, and A. M. Elbashir, “Optimum thermal design of humidification dehumidification desalination systems,” *Desalination*, vol. 349, pp. 10–21, 2014.
- [42] N. Kh, M. Mehdi, and S. Al-hallaj, “Solar desalination based on humidi ® cation processDI . Evaluating the heat and mass transfer coe cients,” vol. 40, pp. 1423–1439, 1999.
- [43] F. Report, R. Mei, and J. Knight, “Innovative Fresh Water Production Process for Fossil Fuel Plants,” no. December, 2006.
- [44] N. Kh, M. Mehdi, A. Aziz, and A. Sabirin, “Solar desalination based on humidi ® cation processDII . Computer simulation,” vol. 40, 1999.
- [45] M. Zamen, M. Amidpour, and S. M. Soufari, “Cost optimization of a solar humidification – dehumidification desalination unit using mathematical programming,” *DES*, vol. 239, no. 1–3, pp. 92–99, 2009.
- [46] “Improvement of Solar Humidification- Dehumidification Desalination Using Multi- Stage Process,” no. January, 2011.
- [47] E. H. Amer, H. Kotb, and G. H. Mostafa, “desalination unit,” vol. 249, pp. 949–959, 2009.
- [48] S. Hou, S. Ye, and H. Zhang, “Performance optimization of solar humidification – dehumidification desalination process using Pinch technology,” vol. 183, no. May, pp. 143–149, 2005.
- [49] S. Hou, “Two-stage solar multi-effect humidification dehumidification desalination process plotted from pinch analysis,” vol. 222, no. 40, pp. 572–578, 2008.
- [50] E. Chafik, “Design of plants for solar desalination using the multi-stage heating / humidifying technique,” vol. 168, pp. 55–71, 2004.
- [51] I. Houcine, M. Benamara, A. Guizani, and M. Maâlej, “Pilot plant testing of a new solar desalination process by a multiple-effect-humidification technique,” vol. 196, no. August 2003, pp. 105–124, 2006.
- [52] J. O *et al.*, “Experimental and theoretical study of a humidification-dehumidification water desalination system using solar energy,” vol. 168, pp. 151–159, 2004.
- [53] C. Yamal, “A solar desalination system using humidification – dehumidification process : experimental study and comparison with the theoretical results f,” vol. 220, pp. 538–551, 2008.
- [54] N. A. S. Elminshawy, F. R. Siddiqui, and M. F. Addas, “Experimental and analytical study on productivity augmentation of a novel solar humidi fi cation – dehumidi fi cation (HDH) system,” vol. 365, pp. 36–45, 2015.

- [55] A. M. A. Dayem and M. Fatouh, “Experimental and numerical investigation of humidification / dehumidification solar water desalination systems,” *DES*, vol. 247, no. 1–3, pp. 594–609, 2009.
- [56] R. K. McGovern, G. P. Thiel, G. P. Narayan, S. M. Zubair, and J. H. L. V., “Performance limits of zero and single extraction humidification-dehumidification desalination systems,” *Appl. Energy*, vol. 102, pp. 1081–1090, 2013.
- [57] H. E. S. Fathb and A. Ghazy, “Solar desalination using humidification-dehumidification technology,” vol. 142, pp. 119–133, 2002.
- [58] G. Wu, H. Zheng, X. Ma, C. Kutlu, and Y. Su, “Experimental investigation of a multi-stage humidification-dehumidification desalination system heated directly by a cylindrical Fresnel lens solar concentrator,” *Energy Convers. Manag.*, vol. 143, pp. 241–251, 2017.
- [59] H. A. Ahmed, I. M. Ismail, W. F. Saleh, and M. Ahmed, “Experimental investigation of humidification-dehumidification desalination system with corrugated packing in the humidifier,” *Desalination*, vol. 410, pp. 19–29, 2017.
- [60] T. Rajaseenivasan and K. Srithar, “Potential of a dual purpose solar collector on humidification dehumidification desalination system,” *Desalination*, vol. 404, pp. 35–40, 2017.
- [61] L. Zhang, W. Chen, and H. Zhang, “Study on variation laws of parameters in air bubbling humidification process,” *Desalin. Water Treat.*, vol. 51, no. 16–18, pp. 3145–3152, Apr. 2013.
- [62] M. T. Ghazal, U. Atikol, and F. Egelioglu, “An experimental study of a solar humidifier for HDD systems,” *Energy Convers. Manag.*, vol. 82, pp. 250–258, 2014.
- [63] C. Muthusamy, M. Gowtham, S. Manickam, M. Manjunathan, and K. Srithar, “Enhancement of productivity of humidification–dehumidification desalination using modified air heater,” *Desalin. Water Treat.*, vol. 56, no. 12, pp. 3294–3304, Dec. 2015.
- [64] E. K. Summers, M. A. Antar, and J. H. Lienhard, “Design and optimization of an air heating solar collector with integrated phase change material energy storage for use in humidification-dehumidification desalination,” *Sol. Energy*, vol. 86, no. 11, pp. 3417–3429, 2012.
- [65] Z. Rahimi-Ahar, M. S. Hatamipour, and Y. Ghalavand, “Experimental investigation of a solar vacuum humidification-dehumidification (VHDH) desalination system,” *Desalination*, vol. 437, no. December 2017, pp. 73–80, 2018.
- [66] M. H. Sharqawy, M. A. Antar, and S. M. Zubair, “Performance evaluation of variable pressure humidification-dehumidification systems,” *Desalination*, vol.

409, pp. 171–182, 2017.

- [67] S. A. Ashrafizadeh and M. Amidpour, “Exergy analysis of humidification-dehumidification desalination systems using driving forces concept,” *Desalination*, vol. 285, pp. 108–116, 2012.
- [68] G. P. Narayan, M. H. Sharqawy, E. K. Summers, J. H. Lienhard, S. M. Zubair, and M. A. Antar, “The potential of solar-driven humidification-dehumidification desalination for small-scale decentralized water production,” *Renew. Sustain. Energy Rev.*, vol. 14, no. 4, pp. 1187–1201, 2010.
- [69] H. Müller-Holst, M. Engelhardt, M. Herve, and W. Schölkopf, “Solarthermal seawater desalination systems for decentralised use,” *Renew. Energy*, vol. 14, no. 1–4, pp. 311–318, 1998.
- [70] “Wire Thermocouple.” [Online]. Available: <http://ratemperaturesensors.co.uk/pfa-flat-pair--exposed-junction-wire-thermocouple-250c-1427-p.asp>. [Accessed: 28-Mar-2018].
- [71] “Panel Mount Flowmeter.” [Online]. Available: <https://www.blue-white.com/f-550-panel-mount-flowmeter/>. [Accessed: 28-Mar-2018].
- [72] “Kestrel 4000 Weather Meter.” [Online]. Available: <https://kestrelmeters.com/products/kestrel-4000-weather-meter>. [Accessed: 28-Mar-2018].
- [73] “Handheld Digital Thermometers.” [Online]. Available: <https://www.omega.com/pptst/HH200A.html>. [Accessed: 28-Mar-2018].
- [74] “Rotary Selector Switches.” [Online]. Available: https://www.omega.com/pptst/OSW_SW14.html. [Accessed: 28-Mar-2018].

APPENDIX A

In this section part of the experimental and theoretical results obtained are presented in tabulated form. The discussion about the results (system performance) covered in chapter 4 with brief comparison between the experimental and theoretical results. From table A.1 to A.11 presents the experimental and theoretical results including total heat input (Q_{in}), humidifier and dehumidifier effectiveness (ϵ_h , ϵ_{dh}), the ratio between the feed water flow rate to air flow rate (MR), top humidifier water temperature, both experimental and theoretical GOR (GOR_{exp} , GOR_{theo}), both experimental and theoretical fresh water production (md_{exp} , md_{theo}).

Table 2: open cold water cycle HDH system performance at humidifier feed water= 3 LPM.

Q_{in} (KW)	ϵ_h	ϵ_{dh}	MR	T7 (°C)	GOR_{exp}	md_{exp} (Kg/s)	GOR_{theo}	md_{theo} (Kg/s)
6.318	0.9486	0.8403	0.6536	72	0.2305	0.000452	0.7074	0.7074
5.657	0.985	0.8178	0.6536	67.5	0.2319	0.000407	0.7464	0.7464
4.976	0.9901	0.7965	0.6525	62.5	0.2024	0.000312	0.7223	0.7223
4.359	0.994	0.4359	0.6513	57.7	0.09555	0.000129	0.6047	0.6047

Table 3: open cold water cycle HDH system performance at humidifier feed water= 3 LPM.

Q_{in} (KW)	ϵ_h	ϵ_{dh}	MR	T7 (°C)	GOR_{exp}	md_{exp} (Kg/s)	GOR_{theo}	md_{theo} (Kg/s)
5.503	0.8542	0.62	0.6639	72.5	0.3094	0.00053	0.8107	0.00185
4.895	0.8964	0.6126	0.6635	67.5	0.2579	0.000392	0.808	0.001638
4.172	0.8979	0.6045	0.6611	62.5	0.2443	0.000316	0.8221	0.001419
3.575	0.99	0.5973	0.6578	58	0.187	0.000207	0.8033	0.001186

Table 4: open cold water cycle HDH system performance at humidifier feed water=4 LPM.

Q_{in} (KW)	ε_h	ε_{dh}	MR	T7 (°C)	GOR _{exp}	md _{exp} (Kg/s)	GOR _{theo}	md _{theo} (Kg/s)
8.452	0.8964	0.7816	0.6688	72.5	0.4095	0.001076	0.8648	0.00303
7.446	0.8907	0.822	0.6676	67.5	0.3152	0.000729	0.8725	0.00269
6.273	0.8017	0.7177	0.6665	62.5	0.2675	0.000521	0.8271	0.002147
5.449	0.6914	0.4376	0.6628	58	0.255	0.000431	0.6942	0.001564
5.031	0.9804	0.4406	0.6613	56	0.2066	0.000322	0.6244	0.001298

Table 5: open cold water cycle HDH system performance at humidifier feed water= 4 LPM.

Q_{in} (KW)	ε_h	ε_{dh}	MR	T7 (°C)	GOR _{exp}	md _{exp} (Kg/s)	GOR _{theo}	md _{theo} (Kg/s)
7.17	0.8252	0.7621	1.014	72	0.2889	0.000646	0.8759	0.002612
5.732	0.7565	0.7498	1.014	67.5	0.2869	0.000512	0.8651	0.002059
5.047	0.7545	0.8019	1.012	62.5	0.2918	0.000458	0.8563	0.001792
4.349	0.8106	0.792	1.012	58.5	0.245	0.000331	0.8849	0.001595

Table 6: open cold water cycle HDH system performance at humidifier feed water= 5 LPM.

Q_{in} (KW)	ε_h	ε_{dh}	MR	T7 (°C)	GOR _{exp}	md _{exp} (Kg/s)	GOR _{theo}	md _{theo} (Kg/s)
10.39	0.6316	0.7847	1.102	72.8	0.42	0.001052	0.9919	0.004298
7.496	0.7051	0.7169	1.1	67.5	0.4006	0.000937	0.9482	0.002957
6.518	0.8275	0.5981	1.1	62.5	0.3364	0.000684	0.9707	0.00263

Table 7: open cold water cycle HDH system performance at humidifier feed water= 5 LPM.

Qin (KW)	ϵ_h	ϵ_{dh}	MR	T7 (°C)	GOR _{exp}	md _{exp} (Kg/s)	GOR _{theo}	md _{theo} (Kg/s)
9.746	0.8149	0.7617	0.7515	71.3	0.46	0.0011	0.9451	0.003831
8.628	0.7856	0.969	0.7515	67.5	0.34	0.000827	0.92	0.003449
8.555	0.99123	0.7456	0.7515	62.5	0.322	0.000805	0.941	0.003504

Table 8: close cold water cycle HDH system performance at humidifier feed water= 3 LPM.

Qin (KW)	ϵ_h	ϵ_{dh}	MR	T7 (°C)	GOR _{exp}	md _{exp} (Kg/s)	GOR _{theo}	md _{theo} (Kg/s)
4.574	0.8175	0.7534	0.7763	62.5	0.4219	0.000599	0.9712	0.001838
4.12	0.795	0.7407	0.7763	57.5	0.3113	0.000398	0.949	0.001617
3.492	0.8327	0.7054	0.7763	52.5	0.2735	0.000296	0.9574	0.001381
2.708	0.8538	0.6535	0.7763	47.5	0.2698	0.000226	0.9904	0.001107

Table 9: close cold water cycle HDH system performance at humidifier feed water= 4 LPM.

Qin (KW)	ϵ_h	ϵ_{dh}	MR	T7 (°C)	GOR _{exp}	md _{exp} (Kg/s)	GOR _{theo}	md _{theo} (Kg/s)
10.17	0.9176	0.9118	1.298	70	0.417	0.001323	0.8087	0.003421
8.355	0.938	0.9171	1.298	66.25	0.3551	0.000924	0.8617	0.00299
6.5	0.9963	0.9211	1.298	59.5	0.3458	0.000699	0.8599	0.002317
6.34	0.999	0.9101	1.298	54.75	0.3402	0.00067	0.7714	0.002026

Table 10: close cold water cycle HDH system performance at humidifier feed water= 3 LPM.

Q_{in} (KW)	ϵ_h	ϵ_{dh}	MR	T7 (°C)	GOR_{exp}	md_{exp} (Kg/s)	GOR_{theo}	md_{theo} (Kg/s)
4.737	0.7817	0.9604	1.87	65	0.3004	0.001323	0.8087	0.003421
3.743	0.7599	0.9669	1.865	60	0.29	0.000924	0.8617	0.00299
2.895	0.7097	0.9678	1.768	55.35	0.2826	0.000699	0.8599	0.002317
2.289	0.6877	0.9629	1.803	52.6	0.1744	0.00067	0.7714	0.002026

Table 11: close cold water cycle HDH system performance at humidifier feed water= 4 LPM.

Q_{in} (KW)	ϵ_h	ϵ_{dh}	MR	T7 (°C)	GOR_{exp}	md_{exp} (Kg/s)	GOR_{theo}	md_{theo} (Kg/s)
6.262	0.449	0.9167	2.012	67.5	0.3692	0.000721	0.9092	0.002368
4.908	0.4431	0.9	1.871	62.5	0.3294	0.000503	0.9161	0.001866
3.861	0.3888	0.864	1.812	57.5	0.2792	0.000335	0.887	0.001419
2.982	0.3896	1.053	1.819	52.5	0.2741	0.000253	0.9208	0.001134

Uncertainty Analysis

It is necessary to evaluate the effect of the measured values on system performance since we are measuring temperature, volumetric flow rates and air speed and humidity. EES provide a tool to provide these analysis, starting the evaluation with knowing that the K-type thermocouples have uncertainty of $\pm 1^{\circ}\text{C}$, Panel mount flow meters which have an uncertainty equal to $\pm 0.5 \text{ LPM}$, a Weather meter is used to measure the speed and humidity of the air with uncertainty of $\pm 0.1 \text{ m/s}$ and 1% respectively and finally a graduated cylinder which measure the fresh water production over a period of time with an accuracy of $\pm 10 \text{ mL}$.

Table 12: Uncertainty analysis for the open cold water cycle HDH system performance at humidifier feed water= 3 LPM.

Q_{in} (KW)	ε_h	ε_{dh}	MR	GOR_{exp}	m_d^{exp} (Kg/hr)
6.318	0.9486	0.8403	0.6536	0.2305 ± 0.1112	1.62648 ± 0.054
5.657	0.985	0.8178	0.6536	0.2319 ± 0.1187	1.46412 ± 0.0543
4.976	0.9901	0.7965	0.6525	0.2024 ± 0.1105	1.1232 ± 0.035
4.359	0.994	0.4359	0.6513	0.09555 ± 0.05574	0.464 ± 0.0011056

Table 13: Uncertainty analysis for the open cold water cycle HDH system performance at humidifier feed water= 3 LPM.

Q_{in} (KW)	ε_h	ε_{dh}	MR	GOR_{exp}	m_d^{exp} (Kg/hr)
5.503	0.8542	0.62	0.6639	0.3094 ± 0.178	1.90656 ± 0.029
4.895	0.8964	0.6126	0.6635	0.2579 ± 0.157	1.41192 ± 0.031
4.172	0.8979	0.6045	0.6611	0.2443 ± 0.166	1.13868 ± 0.027
3.575	0.99	0.5973	0.6578	0.187 ± 0.178	0.74592 ± 0.013

Table 14: Uncertainty analysis for the open cold water cycle HDH system performance at humidifier feed water=4 LPM.

Qin (KW)	ε_h	ε_{dh}	MR	GOR _{exp}	md _{exp} (Kg/hr)
8.452	0.8964	0.7816	0.6688	0.4095 ± 0.147	3.8736 ± 0.099
7.446	0.8907	0.822	0.6676	0.3152 ± 0.121	2.62332 ± 0.059
6.273	0.8017	0.7177	0.6665	0.2675 ± 0.116	1.87416 ± 0.042
5.449	0.6914	0.4376	0.6628	0.255 ± 0.120	1.55088 ± 0.029
5.031	0.9804	0.4406	0.6613	0.2066 ± 0.102	1.15992 ± 0.016

Table 15: Uncertainty analysis for the open cold water cycle HDH system performance at humidifier feed water= 4 LPM.

Qin (KW)	ε_h	ε_{dh}	MR	GOR _{exp}	md _{exp} (Kg/hr)
7.17	0.8252	0.7621	1.014	0.2889 ± 0.126	2.32668 ± 0.05
5.732	0.7565	0.7498	1.014	0.2869 ± 0.151	1.84356 ± 0.028
5.047	0.7545	0.8019	1.012	0.2918 ± 0.164	1.6488 ± 0.0199
4.349	0.8106	0.792	1.012	0.245 ± 0.153	1.19196 ± 0.0298

Table 16: Uncertainty analysis for the open cold water cycle HDH system performance at humidifier feed water= 5 LPM.

Q_{in} (KW)	ε_h	ε_{dh}	MR	GOR_{exp}	m_d^{exp} (Kg/hr)
10.39	0.6316	0.7847	1.102	0.42 ± 0.055	3.78828 ± 0.025
7.496	0.7051	0.7169	1.1	0.4006 ± 0.16	3.37248 ± 0.049
6.518	0.8275	0.5981	1.1	0.3364 ± 0.145	2.4606 ± 0.039

Table 17: Uncertainty analysis for the open cold water cycle HDH system performance at humidifier feed water= 5 LPM.

Q_{in} (KW)	ε_h	ε_{dh}	MR	GOR_{exp}	m_d^{exp} (Kg/hr)
9.746	0.8149	0.7617	0.7515	0.46 ± 0.1	3.96 ± 0.042
8.628	0.7856	0.969	0.7515	0.34 ± 0.104	2.97684 ± 0.0425
8.555	0.99123	0.7456	0.7515	0.322 ± 0.0949	2.898 ± 0.39744

Table 18: Uncertainty analysis for the close cold water cycle HDH system performance at humidifier feed water= 3 LPM.

Q_{in} (KW)	ε_h	ε_{dh}	MR	GOR_{exp}	m_d^{exp} (Kg/hr)
4.574	0.8175	0.7534	0.7763	0.4219 ± 0.24	2.15604 ± 0.04
4.12	0.795	0.7407	0.7763	0.3113 ± 0.1877	1.43136 ± 0.03
3.492	0.8327	0.7054	0.7763	0.2735 ± 0.181	1.0656 ± 0.042
2.708	0.8538	0.6535	0.7763	0.2698 ± 0.219	0.81396 ± 0.054

Table 19: Uncertainty analysis for the close cold water cycle HDH system performance at humidifier feed water= 4 LPM.

Q_{in} (KW)	ε_h	ε_{dh}	MR	GOR_{exp}	m_d^{exp} (Kg/hr)
10.17	0.9176	0.9118	1.298	0.417 ± 0.112	4.7628 ± 0.059
8.355	0.938	0.9171	1.298	0.3551 ± 0.113	3.32784 ± 0.035
6.5	0.9963	0.9211	1.298	0.3458 ± 0.132	2.51604 ± 0.033
6.34	0.999	0.9101	1.298	0.3402 ± 0.121	2.41272 ± 0.0285

Table 20: Uncertainty analysis for the close cold water cycle HDH system performance at humidifier feed water= 3 LPM.

Qin (KW)	ε_h	ε_{dh}	MR	GOR_{exp}	md_{exp} (Kg/hr)
4.737	0.7817	0.9604	1.87	0.3004 ± 0.189	1.59912 ± 0.03
3.743	0.7599	0.9669	1.865	0.29 ± 0.215	1.21788 ± 0.027
2.895	0.7097	0.9678	1.768	0.2826 ± 0.264	0.91656 ± 0.022
2.289	0.6877	0.9629	1.803	0.1744 ± 0.21	0.44676 ± 0.0149

Table 21: Uncertainty analysis for the close cold water cycle HDH system performance at humidifier feed water= 4 LPM.

Qin (KW)	ε_h	ε_{dh}	MR	GOR_{exp}	md_{exp} (Kg/hr)
6.262	0.449	0.9167	2.012	0.3692 ± 0.178	2.59668 ± 0.05
4.908	0.4431	0.9	1.871	0.3294 ± 0.1922	1.81152 ± 0.02
3.861	0.3888	0.864	1.812	0.2792 ± 0.197	1.206 ± 0.14
2.982	0.3896	1.053	1.819	0.2741 ± 0.24	0.91152 ± 0.16

APPENDIX B

In this section we show the ambient condition during which the system was tested, also the temperature, volumetric flow rates, and air properties variation across the system is presented.

Table 22: Test condition for open cold water cycle HDH system at humidifier feed water= 3 LPM.29/7/2018.

Time (mins)	11	11	17	54
V _{md} (mL)	300	270	320	420
T1 (°C)	39.5	37.2	36.5	35.4
T2 (°C)	51	48	49.5	51.3
T4 (°C)	52.2	51	50.2	52.4
T5 (°C)	77	71.9	66.6	54.4
T7 (°C)	70	65	60	55.4
T8 (°C)	31.8	30.2	30.8	31.4
T9 (°C)	31.8	30.4	30.7	31.8
T10 (°C)	32.9	31.1	30.8	31.8
T11 (°C)	33.9	31.9	31.2	31.7
T12 (°C)	37	37	36.5	36
T14 (°C)	48.1	44	42.6	41.2
T15 (°C)	35.2	32	33.8	34.3
T16 (°C)	32.8	30.4	32.2	32.9
T17 (°C)	37	34.8	34.8	35.9
Q _{w1} (LPM)	3	3	3	3
Q _{w2} (LPM)	3	3	3	3
Q _{w4} (LPM)	3	3	3	3
Q _{w5} (LPM)	8	8	8	8
Q _{w6} (LPM)	6	6	6	6
V _{ain avg} (m/s)	0.4	0.4	0.4	0.4
Φ _{ain avg} (%)	0.1825	0.1825	0.1825	0.1825
T _{ain} (°C)	40	39.5	39	38
V _{aoutavg} (m/s)	0.27	0.27	0.27	0.27
Φ _{aoutavg} (%)	0.536	0.5427	0.538	0.564
T _{aout} (°C)	32	31	31	32.5

Table 23: Test condition for open cold water cycle HDH system at humidifier feed water= 3 LPM. 18/7/2018.

Time (mins)	20	19	22	44
V _{md} (mL)	640	450	420	550
T1 (°C)	44.4	42.2	40.4	39
T2 (°C)	51.8	50.3	50.9	47
T4 (°C)	52	51.7	52	48.3
T5 (°C)	74	68.7	63.3	58.4
T7 (°C)	70	65	60	56
T8 (°C)	31.4	32	31.8	31.8
T9 (°C)	31.4	32	31.8	31.7
T10 (°C)	33.6	33.8	32.4	32.9
T11 (°C)	34.6	34.6	33	32
T12 (°C)	40.3	39.8	39.2	37
T14 (°C)	51.8	47.9	47	41.8
T15 (°C)	36.8	36.1	35.5	34.8
T16 (°C)	35.4	34.2	33.6	32.4
T17 (°C)	43.6	43	40.7	35.4
Q _{w1} (LPM)	3	3	3	3
Q _{w2} (LPM)	3	3	3	3
Q _{w4} (LPM)	3	3	3	3
Q _{w5} (LPM)	8	8	8	8
Q _{w6} (LPM)	6	6	6	6
V _{ain avg} (m/s)	0.38	0.38	0.38	0.38
Φ _{ain avg} (%)	0.2843	0.2843	0.2843	0.2843
T _{ain} (°C)	36	36.5	37	37
V _{aoutavg} (m/s)	0.21	0.21	0.21	0.21
Φ _{aoutavg} (%)	0.6226	0.6226	0.6226	0.6226
T _{aout} (°C)	35	34.8	33.9	33

Table 24: Test condition for open cold water cycle HDH system at humidifier feed water= 4 LPM.
4/8/2018.

Time (mins)	6	10	14	20	36
V _{md} (mL)	390	440	440	520	700
T1 (°C)	40.1	39.4	38.9	38	37.9
T2 (°C)	51	51.5	53	56.2	53
T4 (°C)	52	52.6	53.6	56.2	54
T5 (°C)	80.6	75.3	70.6	65	60
T7 (°C)	70	65	60	56	56
T8 (°C)	30.5	31.2	31.6	31.8	32
T9 (°C)	30.6	31.2	31.7	31.8	32
T10 (°C)	32.4	32.8	32.7	32.4	33.1
T11 (°C)	33.6	33.6	33.4	33	33.3
T12 (°C)	38.5	38	37.6	35	36.3
T14 (°C)	49.9	48.8	47.2	45.2	44.4
T15 (°C)	39.8	35.2	35.8	35.3	36.1
T16 (°C)	32.5	32.8	33.8	34.3	35
T17 (°C)	41.7	41.2	44.2	41.8	30.3
Q _{w1} (LPM)	4	4	4	4	4
Q _{w2} (LPM)	4	4	4	4	4
Q _{w4} (LPM)	4	4	4	4	4
Q _{w5} (LPM)	8	8	8	8	8
Q _{w6} (LPM)	6	6	6	6	6
V _{ain avg} (m/s)	0.5	0.5	0.5	0.5	0.25
Φ _{ain avg} (%)	0.3225	0.37	0.46	0.5	0.515
T _{ain} (°C)	39	38	37.5	36.8	36.5
V _{aoutavg} (m/s)	0.31	0.31	0.31	0.31	0.31
Φ _{aoutavg} (%)	0.714	0.72	0.771	0.795	0.782
T _{aout} (°C)	33	32.5	33.5	34	34.5

Table 25: Test condition for open cold water cycle HDH system at humidifier feed water= 4 LPM.9/8/2018.

Time (mins)	11	21	30	20
V _{md} (mL)	430	650	830	400
T1 (°C)	46.8	45.6	42.6	41.5
T2 (°C)	52	57.7	52.7	48.9
T4 (°C)	53	58.2	52.9	50.4
T5 (°C)	75.8	69.3	63	59.3
T7 (°C)	70	65	60	57
T8 (°C)	32.3	33.2	34.6	34
T9 (°C)	32.3	33.3	34.7	34
T10 (°C)	32.4	34.7	35.7	35
T11 (°C)	34.2	32.9	36.1	35
T12 (°C)	38	39.4	38.6	37.5
T14 (°C)	49.7	49.8	46.6	46.6
T15 (°C)	36.6	35.6	35.1	35.1
T16 (°C)	31.9	35.2	34.8	34.8
T17 (°C)	46.2	47.2	43.1	43.1
Q _{w1} (LPM)	4	4	4	4
Q _{w2} (LPM)	4	4	4	4
Q _{w4} (LPM)	4	4	4	4
Q _{w5} (LPM)	8	8	8	8
Q _{w6} (LPM)	6	6	6	6
V _{ain avg} (m/s)	0.33	0.33	0.33	0.33
Φ _{ain avg} (%)	0.188	0.188	0.188	0.188
T _{ain} (°C)	40	40	39.5	39.5
V _{aoutavg} (m/s)	0.173	0.173	0.173	0.173
Φ _{aoutavg} (%)	0.6	0.6	0.6	0.6
T _{aout} (°C)	38.5	38	37	37

Table 26: Test condition for open cold water cycle HDH system at humidifier feed water= 5 LPM. 11/9/2018.

Time (mins)	23	12	15
V _{md} (mL)	850	680	620
T1 (°C)	46	46	41.3
T2 (°C)	57	60	63.3
T4 (°C)	57	60	63.6
T5 (°C)	75.8	69.3	63
T7 (°C)	70	65	60
T8 (°C)	31.7	32	32
T9 (°C)	31.7	32	32
T10 (°C)	43	41.4	37.5
T11 (°C)	44.6	42.8	38.8
T12 (°C)	49.2	47.8	43.6
T14 (°C)	58	54	49.3
T15 (°C)	43.2	41.8	37.7
T16 (°C)	43	41.8	37.4
T17 (°C)	50.2	46	41.4
Q _{w1} (LPM)	3	3	3
Q _{w2} (LPM)	5	5	5
Q _{w4} (LPM)	5	5	5
Q _{w5} (LPM)	8	8	8
Q _{w6} (LPM)	6	6	6
V _{ain avg} (m/s)	0.38	0.38	0.38
Φ _{ain avg} (%)	0.6225	0.5725	0.5725
T _{ain} (°C)	37	37.5	37
V _{aoutavg} (m/s)	0.2	0.2	0.2
Φ _{aoutavg} (%)	0.91	0.91	0.885
T _{aout} (°C)	37	37	37

Table 27: Test condition for open cold water cycle HDH system at humidifier feed water= 5 LPM. 31/12/2017.

Time (mins)	14	14	15
V _{md} (mL)	830	700	730
T1 (°C)	42.9	40.4	33.5
T2 (°C)	56.2	60	58
T4 (°C)	57	61.4	58.6
T5 (°C)	75	72.2	67.5
T7 (°C)	70	65	60
T8 (°C)	35	36.5	37
T9 (°C)	35	36.5	37
T10 (°C)	38	39.5	39.8
T11 (°C)	39	40.2	40.5
T12 (°C)	49.3	50.3	43.3
T14 (°C)	55.6	52.6	40.3
T15 (°C)	40.8	39.6	28.6
T16 (°C)	38.8	37.5	26.2
T17 (°C)	47.8	44	30
Q _{w1} (LPM)	2	2	2
Q _{w2} (LPM)	5	5	5
Q _{w4} (LPM)	5	5	5
Q _{w5} (LPM)	8	8	8
Q _{w6} (LPM)	6	6	6
V _{ain avg} (m/s)	0.56	0.56	0.56
Φ _{ain avg} (%)	0.4	0.4	0.4
T _{ain} (°C)	40	40	40
V _{aoutavg} (m/s)	0.3	0.3	0.3
Φ _{aoutavg} (%)	0.83	0.8	0.77
T _{aout} (°C)	38.5	38	37

Table 28: Test condition for close cold water cycle HDH system at humidifier feed water= 3 LPM.25/3/2018.

Time (mins)	13	15	14	11
V _{md} (mL)	470	360	250	150
T ₁ (°C)	30.9	29.8	28.6	29
T ₂ (°C)	33.2	31.9	30.7	31.1
T ₄ (°C)	36.9	35.2	33.9	34.2
T ₅ (°C)	75.8	70.8	66	61.9
T ₇ (°C)	60	55	50	45
T ₈ (°C)	24.1	25.7	25.8	26.1
T ₉ (°C)	24.2	25.7	25.9	26.2
T ₁₀ (°C)	26.2	26.3	26	27.3
T ₁₁ (°C)	26.8	26.6	26.2	27.8
T ₁₂ (°C)	28	28	28	28
T ₁₄ (°C)	35.2	32.8	31.6	30.8
T ₁₅ (°C)	25.9	25.8	25.3	26.4
T ₁₆ (°C)	30	30	30	30
T ₁₇ (°C)	34.9	33.2	31	30.7
Q _{w1} (LPM)	2	2	1	1
Q _{w2} (LPM)	3	3	3	3
Q _{w4} (LPM)	3	3	3	3
Q _{w5} (LPM)	8	8	8	8
Q _{w6} (LPM)	6	6	6	6
V _{ain avg} (m/s)	0.26	0.26	0.26	0.26
Φ _{ain avg} (%)	0.60325	0.60325	0.60325	0.60325
T _{ain} (°C)	28	28	28	28
V _{aoutavg} (m/s)	0.19725	0.19725	0.19725	0.19725
Φ _{aoutavg} (%)	73.2	75.5	72.4	72.6
T _{aout} (°C)	30	30	30	30

Table 29: Test condition for close cold water cycle HDH system at humidifier feed water= 4 LPM.

Time (mins)	10	17	18	21
V _{md} (mL)	800	950	760	850
T1 (°C)	28.3	30.5	30	27.5
T2 (°C)	36.5	33.8	42	42
T4 (°C)	36.5	39	42	42
T5 (°C)	70	61.6	56.6	53
T7 (°C)	70	62.5	56.5	53
T8 (°C)	24.7	26.5	26.8	26.6
T9 (°C)	24.8	26.6	26.8	26.4
T10 (°C)	26.8	27.8	27.8	27
T11 (°C)	29	29.2	28.6	27
T12 (°C)	33.5	33	31.5	29.5
T14 (°C)	46	42	39.5	35
T15 (°C)	26.4	25.5	23.5	26
T16 (°C)	24	24.7	25	25
T17 (°C)	35.5	33.5	31.5	28.5
Q _{w1} (LPM)	2	1	1	1
Q _{w2} (LPM)	4	4	4	4
Q _{w4} (LPM)	4	4	4	4
Q _{w5} (LPM)	8	8	8	8
Q _{w6} (LPM)	6	6	6	6
V _{ain avg} (m/s)	0.22	0.22	0.22	0.22
Φ _{ain avg} (%)	0.245	0.245	0.245	0.245
T _{ain} (°C)	29	29	29	29
V _{aoutavg} (m/s)	0.1365	0.1365	0.1365	0.1365
Φ _{aoutavg} (%)	0.715	0.675	0.6985	0.517
T _{aout} (°C)	30	30	29	29

Table 30: Test condition for close cold water cycle HDH system at humidifier feed water= 3 LPM.

Time (mins)	16	22	26	40
V _{md} (mL)	430	450	400	300
T1 (°C)	40	39.8	39.7	39.7
T2 (°C)	45.2	46.7	48	49.9
T4 (°C)	47.9	48.4	49.8	52
T5 (°C)	73	67	61.3	57
T7 (°C)	63	57	53.7	51.5
T8 (°C)	29.4	30.6	31.3	32
T9 (°C)	29.4	30.6	31.4	32
T10 (°C)	30	31.8	32.4	32.1
T11 (°C)	30.9	31.3	32.6	32.1
T12 (°C)	34.8	34.4	33.6	33.5
T14 (°C)	46.8	45	44	44.9
T15 (°C)	32.8	33.2	33.7	35.7
T16 (°C)	30.9	31.5	32	33.7
T17 (°C)	41	40.4	40	39
Q _{w1} (LPM)	3	3	3	3
Q _{w2} (LPM)	3	3	33	3
Q _{w4} (LPM)	3	3	3	3
Q _{w5} (LPM)	8	8	8	8
Q _{w6} (LPM)	6	6	6	6
V _{ain avg} (m/s)	0.133	0.133	0.14	0.137
Φ _{ain avg} (%)	0.517	0.517	0.517	0.517
T _{ain} (°C)	33.5	33	33	33
V _{aoutavg} (m/s)	0.1	0.1	0.11	0.105
Φ _{aoutavg} (%)	0.787	0.799	0.7833	0.764
T _{aout} (°C)	35	34.5	34	34

Table 31: Test condition for close cold water cycle HDH system at humidifier feed water= 4 LPM.

Time (mins)	15	11	24	42	36
V _{md} (mL)	650	480	730	850	550
T1 (°C)	43	43	42.7	41.2	40
T2 (°C)	45	44.4	44.6	45.7	47.5
T4 (°C)	47	46.5	46.6	47.1	48.5
T5 (°C)	67	62.5	56.7	50.7	49
T7 (°C)	70	65	60	55	50
T8 (°C)	26.8	27.4	28.7	29.6	29
T9 (°C)	26.8	27.3	28.7	29.8	29
T10 (°C)	27.5	28.6	28.9	29.7	29
T11 (°C)	29.4	29.9	29.8	30.4	30.1
T12 (°C)	29	27.7	27	26.6	25.8
T14 (°C)	43.8	45.1	45.1	44	43.8
T15 (°C)	29.2	30	31.8	33.6	33.6
T16 (°C)	31.3	30.6	32	33	33.5
T17 (°C)	51.5	47.6	46.4	44.5	43.2
Q _{w1} (LPM)	4	4	4	4	4
Q _{w2} (LPM)	4	4	4	4	4
Q _{w4} (LPM)	4	4	4	4	4
Q _{w5} (LPM)	8	8	8	8	8
Q _{w6} (LPM)	6	6	6	6	6
V _{ain avg} (m/s)	0.167	0.16	0.172	0.177	0.176
Φ _{ain avg} (%)	0.449	0.469	0.505	0.565	0.55
T _{ain} (°C)	27.5	27.5	27.5	26.5	26
V _{aoutavg} (m/s)	0.14	0.127	0.147	0.155	0.154
Φ _{aoutavg} (%)	0.913	0.917	0.8887	0.824	0.80
T _{aout} (°C)	28.5	31	31	32	32

APPENDIX C

Photos for all measuring devices in the step shown in this section.



Figure 34: Thermocouple. [70]



Figure 35: Flow meter. [71]



Figure 36: Weather meter. [72]



Figure 37: Digital thermometer. [73]



Figure 38: Rotary Thermocouple Selector Switches. [74]

Vitae

Name : Mohammed Elmounzir Isam Eldin Bashir

Nationality : Sudanese

Date of Birth : 6/4/1990

Email : elmounzir@hotmail.com

Address : Algreaf Block 81 House NO. 87, Khartoum, Sudan.

Academic Background : B.Sc. (honor) in mechanical Engineering from university of Khartoum, October 2012.

Projects : Design cooling system using solar energy for AmiPharma factory, Sudan.

A Thesis submitted and presented as partial fulfillment of
B.Sc. (Hon) in Mechanical Engineering.